Environ Geochem Health (2020) 42:4011–4036
https://doi.org/10.1007/s10653-020-00660-w

ORIGINAL PAPER

Assessing the geochemical and environmental baseline of heavy metals in soils around hydrothermal hematite–barite–galena veins in Baghin area, Kerman, Iran

Arezoo Alizadeh-Kouskuie · Habibeh Atapour · Farah Rahmani

Received: 24 February 2020 / Accepted: 1 July 2020 / Published online: 16 July 2020

Abstract To assess the geochemical and environmental baseline as well as the availability of the heavy elements in soils around the hematite–barite–galena veins in the Baghin area, a total of 70 soil samples were collected and analyzed by ICP-OES for 43 heavy metals and metalloids. Compared to the global soil level or crustal abundance, the calcareous soils are 2–26 magnitudes enriched in Ca, Cu, Pb, Zn, Cd, Se, As, Sb and Sr. The ferruginous soils are highly enriched in Fe, Mo, Pb, Zn, Cd, As, Sb, Ba and Sr, almost 2–49 orders higher than the crustal abundance and global soil level. Additionally, the baritic soils are 3–94 times higher than the crustal and global soil values for Ba, Cu, Mo, Pb, Zn, Ni, Co, Cd, Se, As, Sb and Sr. However, the soils developed on the shale layers are moderately enriched in As, Zn, Se, Sb, Ba, Pb and Sr. The high concentrations of heavy metals are possibly related to the presence of minor sulfide minerals in barite–rich soils or adsorption by Fe-oxy-hydroxides formed by oxidation of sulfide minerals. Therefore, the oxidation of minor sulfide minerals in barite veins may be prone to acid mine generation and of environmental concern. The inhalation of silica dusts released by silica–rich barite ores (20% SiO_2) during crushing, milling, as well as using in drilling mud may trigger silicosis. Despite the high baseline values of some heavy metals and metalloids, the presence of Fe-oxy-hydroxides and clay minerals in the soils could play significant roles in sequestering the toxic effects of heavy metals contamination in soil, groundwater, plants, wildlife and humans.

Keywords Geochemical baseline of heavy metals · Hematite–barite–galena veins · Environmental availability and soil fertility · Baghin area

A. Alizadeh-Kouskuie · H. Atapour (✉)
Department of Mining Engineering, Faculty of Engineering, Shahid Bahonar University of Kerman, Kerman, Iran
e-mail: atapour@uk.ac.ir

A. Alizadeh-Kouskuie
e-mail: a.alizadeh.k2016@gmail.com

F. Rahmani
Medical Geology Center, Geological Survey of Iran, Tehran, Iran
e-mail: farahrahmany@yahoo.com

Introduction

Soils developed on mineralized host rocks of the barite-rich Mississippi Valley-Type (MVT), sedex and massive sulfide ores are characterized by high values of heavy metals (Fe, Cu, Zn, Pb, Cd), metalloids (As, Sb, Se) and other major and trace elements (Filipek and Plumlee 1999). In this regard, the normal background concentrations of the elements are modified due to the geogenic hydrothermal mineralization and alteration. Despite considerable invaluable geochemical data on the environmental geochemistry of base

metal sulfide ores, less attention has been given to the geochemical and environmental assessment of heavy metals around the hematite–barite–galena mineralization. The exploration, mineralization, mining and metallurgical processing and environmental assessment of barite associated with base metal sulfide minerals could generate potentially toxic heavy metals, metalloids and sulfates into soils, sediments and groundwater (Simini et al. 2002; Vlaardingen et al. 2005; Suresh et al. 2007; Menzie et al. 2008; Oden 2012; Lamb et al. 2013; Zarei et al. 2014; Adamu et al. 2015; Shahab et al. 2016). The bioavailability and toxicity of barite ores in soils and plants have been noticed by Simini et al. (2002) and Lamb et al. (2013), who suggested that barite ores may contaminate water, soil and plants.

Although there are more than 33 barite mines (Fig. 1) in Iran (Ganji 2015), no environmental investigation has been proposed, regarding the geochemical baseline of heavy metals and metalloids in soil and their environmental impacts around the barite deposits.

In this investigation, a total of 70 soil samples were collected and analyzed by ICP-OES for total concentrations of 43 elements (Al, Ti, Fe, Mg, Ca, Na, K, P, Mn, Ba, Rb, Sr, Cu, Mo, Pb, Zn, Ni, Co, Cr, Cd, V, Se, Li, Cs, Zr, W, As, Sb, Bi, Be, Ga, Nb, Se, Y, Ce, Nd, Sm, Eu, Gd, Dy, Er, Yb). The details of methodology, regarding the samples and analysis will be described in the section of sampling and analysis. The main objectives of this investigation are as follows: (1) to determine the geochemical baseline of heavy metal concentrations in soils developed on carbonate rocks, shale and hydrothermal barite–hematite–galena veins; (2) to assess the bioavailability, and soil fertility implications of heavy metals released from rock to soil during chemical weathering and soil formation; (3) to assess the possible contamination and hazardous impacts caused by the heavy metals, metalloids and other elements.

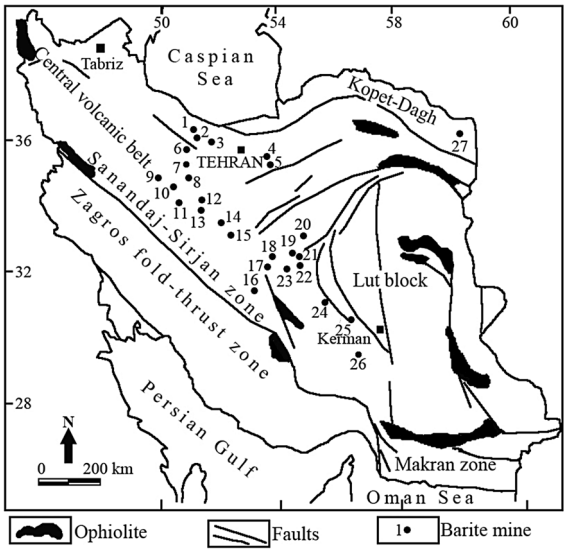

Fig. 1 Structural map of Iran, showing distribution of the most distinguished barite deposits [Modified from Kashfi (1997); Aghanabati (2004); Rajabzadeh (2007); Ehya (2012); Ghorbani (2013); Zarasvandi et al. (2014)]. (1) Elite, (2) Seplark, (3) Ardekan, (4) Garmab, (5) Chah Shirin, (6) Dasht-e Deh, (7) Chenarvardeh, (8) Bijgan, (9) Tang-abad, (10) Jasb, (11) Tappeh-sorkh Bichegan, (12) Vavan, (13) Darreh Kashan, (14) Kamshacheh, (15) Farseh, (16) Khaneh Hozeh-abad, (17) Haft-har, (18) Hoodeh, (19) Lar, (20) Haji Abad, (21) Ahoorak Taleghen, (22) Dorbid, (23) Niyook, (24) Chari-Abtorsh, (25) Baghin, (26) Goly Choupaan, (27) Ghara Gheytan

Geological setting and distribution of barite deposits in Iran

As shown in Fig. 1, the most important barite deposits mostly occur in central Iran and Sanandaj–Sirjan zone (Aftabi and Abbasnejad 1990; Kashfi 1997; Khoshjou 1999; Rajabzadeh 2007; Gholami 2011; Ghorbani 2013; Zarasvandi et al. 2014; Haji Babaei and Ganji 2018). The total reserve of barite deposits in Iran is estimated to be about 122 Mt (Ganji 2015). The barite deposits of Late Precambrian–Early Cambrian in Iran are known in Alborz and Azerbaijan area. Fluorine-bearing barite deposits of Permian and Triassic age have been reported in Komeshcheh (Rajabzadeh 2007), Farsesh (Zarasvandi et al. 2014), Aligodarz (Khoshjou 1999; Zaheri-Abdehvand et al. 2012), central Iran and Alborz (Elika, Donna and Pachi Miana) (Khoshjou 1999; Zaheri-Abdehvand et al. 2012). The barite deposits of Cretaceous age were mostly formed in central Iran and Sanandaj–Sirjan zone and often are associated with lead and zinc deposits in Mehdi Abad and Malayer–Isfahan structural zone. Tertiary barite deposits are located in central Alborz, Azarbaijan and Orumieh-Dokhtar [Qom, Saveh, Kashan, Delijan and Qazvin, Khoshjou (1999)]. These deposits are mostly associated with volcanic and volcano-sedimentary rocks and formed

as stratiform, lens shape and hydrothermal vein deposits (Ghorbani 2013). Also, hematite–barite hydrothermal vein deposits of Tertiary age have been reported in Ahmadabad, northeast of Semnan, Iran (Haji Babaei and Ganji 2018).

In Kerman province, the barite deposits are located in Chah Makaan-Chari Baghin area (Aftabi and Abbasnejad 1990), Abtorsh (Kashfi 1997) and Bolbulouieh (Porchangiz 2011) areas. Other vein-type hydrothermal barite–hematite–galena deposits have also been reported in Gaz Dareh, Abtrosh, Arjasb, Estakhroeiah-Arjasb, Kuh-e-Gabri, Daarssinoieh, northwest of Baghin, northeast of Kerman, (Gholami 2011 and Zienalipour-Heidarabadi 2011).

Geology and climatology

The studied area is a part of Baghin geological map 1:100,000 scale, Kerman province, southeastern Iran at 56°30′ and 56°35′E and 30°22′ and 30°26′N (Fig. 2). The maximum and minimum annual temperatures in the area are 37 °C (July) and 8 °C (January), respectively (Atapour 2015). Average annual rainfall in the study area is about 149.1 mm, which mainly takes place between November and March; thus, the climate is classified as arid–semiarid climate type (Atapour 2015). The prevailing wind direction in this area is west and northwest (Hamzeh et al. 2011).

Based on geological investigation (Djokovic and Dimitrijevic 1972; Alizadeh-Kouskuie 2019), the area is composed of different geological rock units that are summarized in Fig. 2. The oldest Paleozoic rock units include Ordovician metamorphic limestone and dark grey marbles that are intruded by hornblende diorite and gabbro intrusive bodies. Silurian–Devonian units are composed of basal reddish brown sandy conglomerate, sandstone, dolomite, dolomitic limestone, shale, phosphatic layers and dark grey limestone with thin dolomitic interlayers. Carboniferous rocks are mainly composed of marl, limestone and dolomite.

The Mesozoic rocks are predominantly composed of sandstone and marl-limestone, shale and quartz sandstones of Jurassic age (Djokovic and Dimitrijevic 1972). These are covered by reefal limestone of Upper Cretaceous age (Huckriede et al. 1962; Atapour and Aftabi 2002; Atapour 2015). Most of the Upper Neogene units include conglomerate, breccia, sandstone, and marl (Djokovic and Dimitrijevic 1972). The most frequent pebbles of the Neogene conglomerate consist of Paleozoic and rarely Jurassic sandstones and carbonate rocks, which formed during post-Alpine orogenic activities in the area (Aftabi and Abbasnejad 1990). The upper part of these units includes grey marl with lenses of gypsum of Pliocene age. According to Dimitrijevic (1973), Atapour and Aftabi (2002), Atapour (2015) and Alizadeh-Kouskuie (2019), the Quaternary units include: (1) alluvial fans, gravel fans, and terraces; (2) sand dune; and (3) alluvial sediments, which are composed of recently transported alluvium from the neighboring bed rocks. The Pleistocene conglomerate covers Jurassic and Cretaceous units (Aftabi and Abbasnejad 1990). Aeolian sands cover southern part of the studied area. Also, there are some outcrops of post-Eocene andesitic and diabasic dikes which have been intruded into the Upper Cretaceous rocks. Structurally, the studied area is formed by a long and narrow anticline and strike-slip faults (Djokovic and Dimitrijevic 1972; Dimitrijevic 1973; Aftabi and Abbasnejad 1990).

Ore mineralization

Hematite–barite–galena mineralization occurs as primary hydrothermal veins crosscutting the carbonate and shale host rocks of Paleozoic–Mesozoic age (Fig. 2) (Aftabi and Abbasnejad 1990; Kashfi 1997; Gholami 2011; Alizadeh-Kouskuie 2019). The vein mineralization is controlled by faults in the host rocks and the thickness of the veins ranges from few centimeters to a meter. Mineralogically, the hydrothermal veins include the following subdivisions: (1) hematite–goethite–siderite–limonite (Fig. 3a), (2) hematite–limonite–barite (Fig. 3b–d) and (3) barite–galena (Fig. 3e), (4) barite and malachite (Fig. 3f) and (5) fluorite–barite–limonite (Fig. 3g) (Aftabi and Abbasnejad 1990; Kashfi 1997; Gholami 2011; Alizadeh-Kouskuie 2019). The purple-blue or violet colored fluorite (Fig. 3g) in the studied area is similar to the Blue John fluorite reported by Galwey et al. (1979).

Other minor minerals include sphalerite and pyrite. Goethite, limonite, malachite and azurite are formed by supergene oxidation of the sulfides, although goethite has also been formed by the hydration of hematite. The ore structures occur mainly as open space fillings in veins and zebra-type barite–galena.

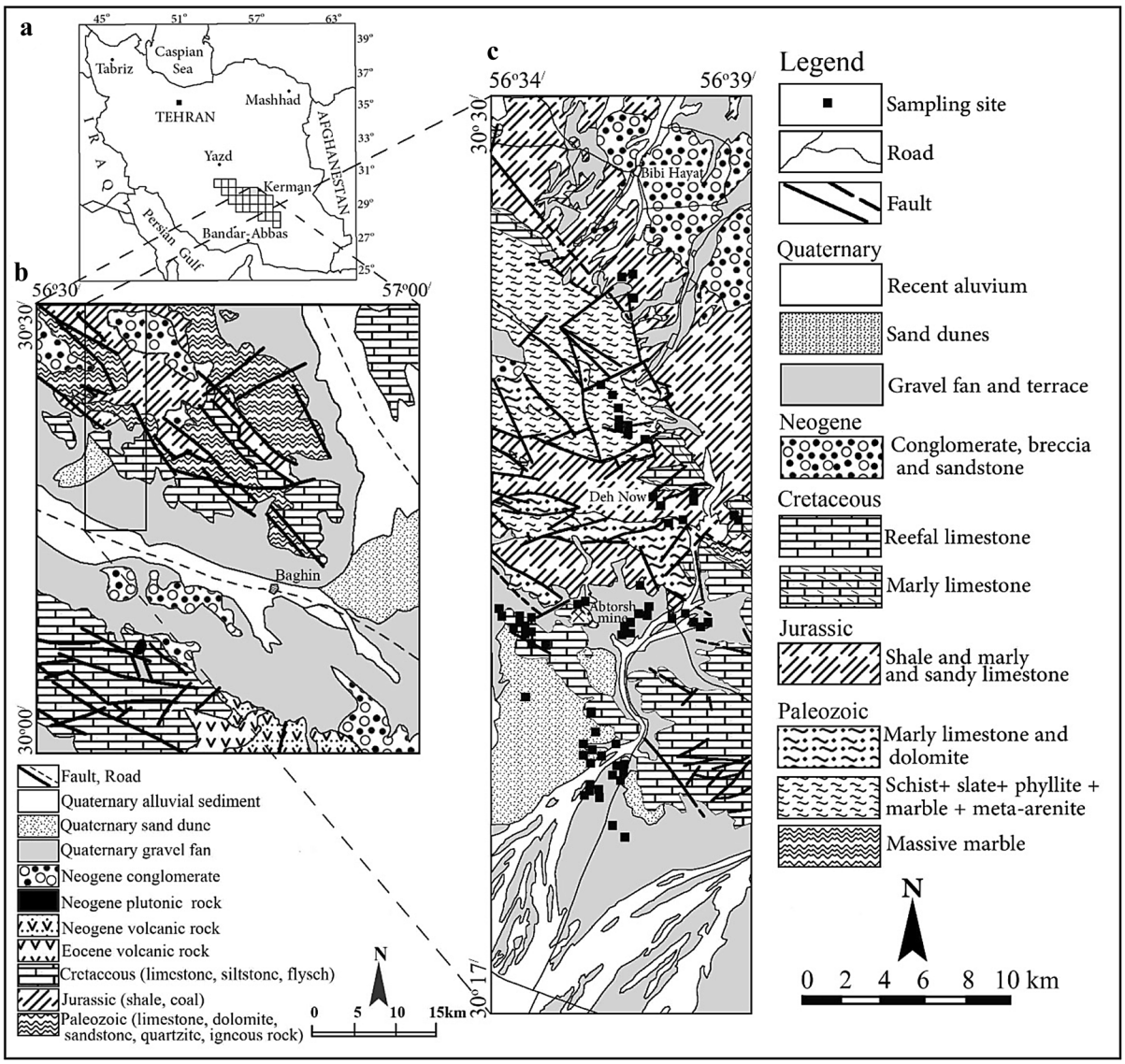

Fig. 2 Geological map of the studied areas of Baghin 1:100,000 scale map, **a** Iran map, **b** simplified map of Baghin 1:100,000 scale map and **c** studied area (modified after Djokovic and Dimitrijevic 1972; Anonymous 2001; Alizadeh-Kouskuie 2019)

The zebra ore structure suggests a Mississippi Valley–Type barite mineralization (Fig. 3e). The average ore grade of Abtorsh mine includes 33% BaO, 15% SO_3, 20% SiO_2, 1.3% Fe_2O_3, 1.6% Pb, 0.2% Zn, 2.2 ppm Cd, and 6.3 ppm Bi, respectively (Kashfi 1997).

Soil formation

Carbonate and shale host–rocks as well as hydrothermal veins have been subjected to chemical weathering processes. Due to the arid–semiarid climate of the area, no distinguished soil horizons are formed. In this regard, the soils are very young and since lack significant profile development, they could be classified as Entisol (USDA 2014). This is reflected by the presence of little modified parent rocks in the soils. Therefore, the most important soils can be subdivided as follows: (1) soils developed on the carbonate rocks (calcareous soils) (Fig. 4a), (2) soils formed on the hydrothermal iron oxide veins (ferruginous soils) (Fig. 4b), (3) soils derived from the weathering of

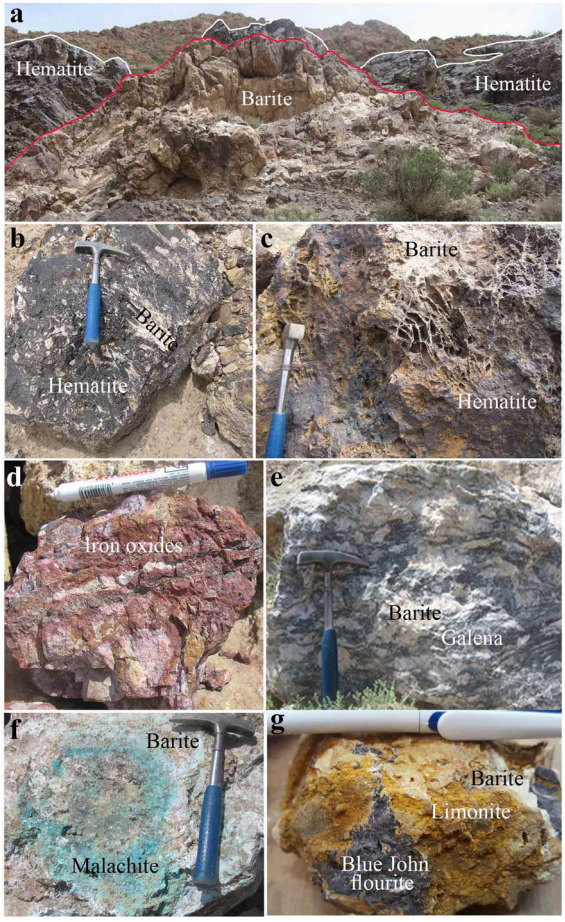

Fig. 3 The outcrops of hydrothermal veins in studied area, **a** hematite and barite veins, **b** association of hematite and barite in veins, **c** boxwork structure in hydrothermal veins, **d** gossanized hematitic and baritic veins, **e** zebra texture and mineralization of galena in baritic veins, **f** malachite mineralization in baritic veins and **g** purple fluorite mineralization in hydrothermal veins, Abtorsh mine

barite veins (baritic soils) (Fig. 4c) and (4) the soils originated from the weathering of shale outcrops (Fig. 4d). The main mineral compositions of the soils are clay minerals, barite, calcite, dolomite, quartz, chert, hematite, goethite, limonite with very minor sulfide minerals. Hematite occurs in primary hydrothermal veins, but goethite is a secondary iron oxide formed as a result of hematite hydration and oxidation of minor sulfide minerals. However, as the soils are of Entisol type, they contain minor fragments of hematite, but with higher modal of goethite. Therefore, they have no relation to either old soil in the mining area or sediments.

Sampling and analytical methods

Soil sampling

The soil samples were performed by random sampling method, which is a flexible design for surveying the average baseline and pollutant concentration of potentially harmful elements (IAEA 2004). The samples were taken in a circle of 1 m in diameter and at 0–5 cm depth (IAEA 2004). Due to the homogenous nature of the soils developed on different host rocks, a total of 70 samples including calcareous soils (20 samples), ferruginous soils (16 samples), baritic soils (14 samples) and soils developed on shale layers (20 samples) were collected. The location of sampling sites is shown on the geological map (Fig. 2).

Analytical methods

The soil samples were powdered to 200 mesh size, fused by lithium metaborate ($LiBO_2$) and cesium chloride (CsCl), decomposed by aqua regia digestion, using designation of EPA International Standards, in particular an American National Standard (2001), and analyzed by ICP-OES method (Varian-Agilent 700 Series) in Applied Research Laboratory of Geological Survey of Iran, Karaj, Iran. The accuracy against the certified reference materials (American National Standard 2001) ranges from 93.84 to 99.81%, respectively. The precision for repeated analysis for different elements is less than 10 percent of the relative standard deviations (RSD %).

Geochemical results

The geochemical results for major and trace elements are shown in Tables 1 and 2 and compared to those of the crustal abundance, carbonate-shale (host rocks in the area), global soil level, soil permissible limits and plant permissible limits. The mean, maximum, minimum, enrichment factor, geo-accumulation index, frequency diagrams as well as box-whisker plot diagrams for the heavy metals in soil samples are also given in Tables 1, 2 and Fig. 5. The statistical parameters were performed by SPSS and Excel software. In order to explore the geochemical and environmental signatures of each element, they are described as the following:

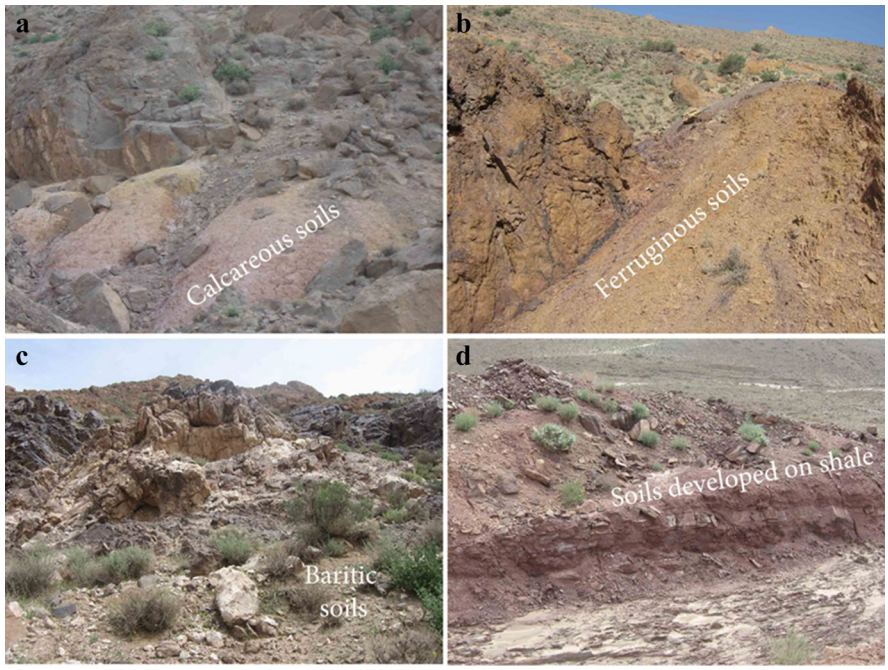

Fig. 4 Field outcrop of the four types of soils in studied area, **a** calcareous soils, **b** ferruginous soils, **c** baritic soils and **d** soils developed on shale layers

Aluminum (Al)

The mean baseline values of aluminum in calcareous soils, ferruginous soils, baritic soils and soils developed on shale layers are 80,502, 54,940, 48,321 and 114,696 mg/kg, respectively (Table 1). These values appear to be almost similar to crustal abundance and global soil level (Lindsay 1979; De Vos and Tarvainen 2006; Salminen et al. 2005). The frequency histogram, box plot and cumulative percentage diagrams (Fig. 5a) show a normal distribution, reflecting four different soil populations. Large quantities of Al in soils occur as aluminosilicates and only easily mobile and exchangeable fractions of Al play an important role in soil fertility (Kabata-Pendias and Mokherjee 2007), although such low level of soluble Al can have beneficial effect on plant growth (Kabata-Pendias 2011) and increase the phosphorus availability as well as alleviating Fe and Mn toxicity (Muhammad et al. 2018). Aluminum has a low mobility under most environmental conditions, although below pH 5.5 its solubility increases as it is released from silicate rocks and may also be mobilized in anionic form under strongly alkaline conditions at pH values above 8 (Shiller and Frilot 1996). Since the aluminum values in different soils are similar to the normal global soil level, no hazardous impact can be expected via plant nutrition in the studied area.

Iron (Fe)

Iron is considered as the fourth abundant heavy metal on the earth crust-soil, an essential nutrient for soil fertility and plant growth, an activator for respiration and plays a significant role in the production of chlorophyll and green color of growing plants (Levinson 1980; Kabata-Pendias 2011; Colombo et al. 2013). The average iron baseline concentration in order of increasing includes 43,162 mg/kg, 50,324 mg/kg, 86,558 mg/kg 136,205 mg/kg in calcareous soils, soils developed on shale layers, baritic soils and ferruginous soils, respectively (Tables 1 and 2), almost 2 magnitudes greater than the crustal abundance and global soil level. The highest baseline value of iron reaches up to 300,000 mg/kg and is related to the ferruginous soils, indicating the presence of hematite, goethite and other Fe-oxy-hydroxide minerals. The frequency histogram, box plot and cumulative percentage diagrams (Fig. 5b) show anomalous positive skewness and lognormal distribution of iron, reflecting four different soil populations. The common range of Fe contents in soils is between 0.1 and 10%, and its distribution in soil profiles is variable and controlled

Table 1 Major, minor and trace elements (mg/kg) in soil samples analyzed by ICP–OES methods in Geological Survey of Iran (Karaj)

Elements		Al	Ti	Fe	Mg	Ca	Na	K	P	Mn	Ba	Rb	Sr
Crustal content		81,300	5700	50,000	20,900	36,300	28,300	25,900	1200	950	425	90	375
Calcareous soils (20)	Mean	80,502	3684	43,162	17,016	129,920	11,831	18,140	637	774	564	84	531
	Max	98,840	7319	60,384	45,574	221,011	16,733	41,463	955	1522	2660	159	887
	Min	38,979	1336	20,877	8903	23,391	2764	8763	316	282	191	43	307
Ferruginous soils(16)	Mean	54,940	2448	136,205	13,822	91,101	11,415	14,530	462	464	889	69	982
	Max	90,054	4170	300,000	25,385	201,168	50,374	28,564	843	948	2660	150	4215
	Min	3510	151	34,627	4788	35,210	383	892	118	0.02	258	8.2	328
Baritic soils (14)	Mean	48,321	1438	86,558	12,783	59,037	5137	13,275	514	1055	1823	55	1886
	Max	166,184	3926	228,419	34,389	187,593	16,383	46,921	1911	2915	2660	153	4332
	Min	1376	189	4519	600	16,451	212	132	73	0.02	266	2.9	286
Soils on shale (20)	Mean	114,697	4410	50,324	12,014	29,527	6246	30,195	562	800	860	148	388
	Max	160,914	5402	66,843	30,899	118,435	24,805	48,629	825	2891	2660	209	2660
	Min	76,362	2571	31,045	6071	3179	2442	16,268	312	118	269	84	119

Elements		Cu	Mo	Pb	Zn	Ni	Co	Cr	Cd	V	Se	Li	Cs	Zr	W	As
Crustal content		55	1.5	12	70	75	25	100	0.2	135	0.05	20	3.0	165	1.5	1.8
Calcareous soils (20)	Mean	67	1.2	41	100	33	14	73	0.4	116	0.2	24	10	151	0.9	26
	Max	665	3.5	130	161	48	20	146	1.7	172	0.8	45	14	194	3.7	140
	Min	14	0.6	9.4	65	17	8.7	33	0.2	48	0.1	9.5	4.3	66	0.5	9.9
Ferruginous soils(16)	Mean	53	6.8	40	106	38	13	55	0.3	96	0.2	19	32	127	0.9	30
	Max	119	28	73	180	50	18	105	0.5	157	0.5	39	120	231	1.9	59
	Min	23	0.5	8.7	40	26	8.3	5.6	0.2	33	0.1	2.7	7.7	28	0.5	4.9
Baritic soils (14)	Mean	290	6.2	45	168	188	51	100	1.0	90	0.4	18	16	75	0.9	114
	Max	1207	37	77	770	2036	478	494	5.7	289	3.6	78	46	196	2.3	800
	Min	17	0.5	14	22	4.5	2.6	4.3	0.2	9.8	0.1	1.1	0.5	12	0.5	4.3
Soils on shale (20)	Mean	39	1.4	39	115	41	18	114	0.4	147	0.3	53	8.8	267	1.4	17
	Max	75	2.9	70	425	55	22.70	163	1.0	201	1.0	108	11.7	393	2.0	33
	Min	6.2	0.7	9.8	32	22	12.15	52	0.2	105	0.1	7.3	5.2	100	0.9	6.4

Elements		Sb	Bi	Be	Ga	Ge	Nb	Sc	Y	Ce	Nd	Sm	Eu	Gd	Dy	Er	Yb
Crustal content		0.2	0.2	2.8	15	1.5	20	16	30	60	28	6.0	1.2	5.4	3.0	2.8	3.0
Calcareous soils (20)	Mean	9.0	0.3	1.4	16	1.8	19	11	19	39	26	4.3	1.1	5.6	3.4	2.1	3.4
	Max	140	0.6	2.7	23	2.5	53	14	22	69	36	6.2	1.3	7.4	4.5	3.8	4.1
	Min	0.8	0.1	0.9	12	1.0	11	5.5	11	22	18	2.5	0.7	3.5	2.2	0.9	1.9
Ferruginous soils(16)	Mean	9.4	0.3	1.8	29	7.9	14	8.5	19	32	23	8.5	1.3	22	4.7	1.4	3.6
	Max	52	0.4	5.8	64	24	19	14	24	69	35	20	2.0	66	11	2.3	5.0
	Min	0.4	0.1	0.5	14	1.3	9.5	1.1	6.2	3.0	11	3.9	0.8	4.8	1.8	0.1	2.8
Baritic soils (14)	Mean	42	0.6	3.7	19	3.9	32	9.2	17	34	22	5.1	1.2	10	3.6	1.7	2.4
	Max	228	2.9	30	36	10	129	35	75	141	54	12	2.7	30	20.5	6.3	5.7
	Min	0.6	0.2	0.1	27	0.4	1.9	0.5	3.2	2.2	5.8	0.5	0.2	0.4	0.2	0.2	0.5
Soils on shale (20)	Mean	1.8	0.5	3.1	24	2.4	25	15	22	76	32	5.8	1.4	6.3	3.3	2.2	3.1
	Max	8.5	0.8	5.5	33	3.6	35	19	33	116	45	6.7	1.8	7.9	7.2	2.7	3.9
	Min	0.5	0.2	1.5	17	1.5	16.9	12	13	46	25	5.0	1.0	4.5	1.4	1.4	2.3

*Faure (1992)

Table 2 The enrichment factor (Ef) and index of geoaccumulation of elements in four types of soils (1 related to crust and 2, global average of soils) (mg/kg)

Elements	Al	Fe	Ca	Cu	Mo	Pb	Zn	Ni	Co	Cr	Cd	Se	As	Sb	Ba	Sr
Crust[1]	81,300	50,000	36,300	55	1.5	12.5	70	7	25	100	0.2	0.05	1.8	0.2	425	375
Soil permissible limits[2]	–	–	–	30	5	60	200	50	20	100	1	–	5	2	750	–
Plant permissible limits[3]	–	–	–	5–30	0.2–1	5–10	27–150	0.1–5	0.02–1	0.1–0.5	0.05–0.2	0.001–2	1–1.7	7–50	–	–
Average global soils[4]	71,000	38,000	13,700	30	2	10	50	25	8	100	0.1	0.3	5	0.5	430	20
Carbonates in the area	5600	37,180	8.0	14	57	21	65	31	9	32	0.2	0.1	78.3	276	57	21
Shale in the area	67,500	85,600	31.9	6	68.4	29.8	32	61.6	12	52	0.3	0.2	76.1	543	68	30
Calcareous soils (20)																
Average	80,502	43,162	129,920	68	1.2	41.08	100	33	14	73	0.4	0.2	26	9.0	564	53
Ef/crust	1	0.9	3.6	1.2	0.8	3.29	1.4	0.4	0.6	0.7	1.9	4.0	14.6	45.2	1.3	1.4
Ef/global soils	1.1	1.1	9.5	2.3	0.6	4.11	2.0	1.3	1.8	0.7	6.3	0.7	5.3	18	1.3	27
Ef/carbonates	14	18	0.4	8.4	–	2.1	1.7	1.6	–	2.3	–	–	–	–	7.2	1.9
Ef/shale	1.2	1.5	1.5	2.1	–	1.9	1.5	1.1	–	1.2	–	–	0.9	–	7.4	1.0
*I*geo/crust	− 0.6	− 0.8	1.3	− 0.3	− 1.0	1.1	− 0.1	− 1.8	− 1.4	− 1.0	0.3	1.4	3.3	4.9	− 0.2	− 0.1
*I*geo/global soils	− 0.4	− 0.4	2.7	0.6	− 1.4	1.5	0.4	− 0.2	0.2	− 1.0	2.1	− 1.2	1.8	3.6	− 0.2	4.2
Ferruginous soils (16)																
Average	54,940	136,205	91,101	52.7	6.8	40	106	38	13	53	0.3	0.2	30	9.4	889	982
Ef/crust	0.7	2.8	2.5	1.0	4.6	3.2	1.5	0.5	0.5	0.6	1.4	4.2	17	47.2	2.1	2.6
Ef/global soils	0.8	3.6	6.7	1.8	3.4	4.0	2.1	1.5	1. 7	0.6	4.5	0.7	6.0	18.9	2.1	49
Ef/carbonates	9.8	56.8	0.3	6.6	–	2.1	1.9	1.8	–	1.8	–	–	–	–	11	3.6
Ef/shale	0.8	4.8	1.1	1.7	–	1.8	1.6	1.3	–	0. 9	–	–	1.0		11.7	1.8
*I*geo/crust	− 1.2	0.9	0.7	− 0.7	1.6	1.1	0.02	− 1.6	− 1.5	− 1.5	− 0.2	1.5	3.5	5.0	0.5	0.8
*I*geo/global soils	− 1.0	1.3	2.2	0.2	1.2	1.4	0.5	0.001	0.2	− 1.5	0.3	− 1.1	2.0	3.7	0.5	5.0
Baritic soils (14)																
Average	48,321	86,558	59,037	290	6.2	45	168	188	51	100	1.0	0.4	114	42	1823	1886
Ef/crust	0.6	1.7	1.6	5.3	4.2	3.6	2.4	2.5	2.0	1.0	4.8	7.2	63	210	4.3	5.0
Ef/global soils	0.7	2.2	4.3	9.7	3.1	4.5	3.4	7.5	6.3	1.0	16	1.2	23	84	4.2	94
Ef/carbonates	8.6	36	0.2	36	–	2.3	2.9	9.2	–	3.2	–	–	–	–	23	6.8
Ef/shale	0.7	3.1	0.7	9.1	–	2.0	2.5	6.3	–	1.6	–		3.8		24	3.5
*I*geo/crust	− 1.3	0.2	0.1	1.8	1.5	1.3	0.7	0.7	0.4	− 0.6	1.7	2.3	5.4	7.1	1.5	1.8
*I*geo/global soils	− 1.1	0.6	1.5	2.7	1.1	1.6	1.2	2.3	2.1	− 0.6	3.4	−0.3	3.9	5.8	1.5	6.0
Soils developed on shale (20)																
Average	114,697	50,324	29,527	39	1.5	39	115	41	18	114	0.4	0.3	17	1.8	856	388
Ef/crust	1.4	1.0	0.8	0.7	1.0	3.1	1.6	0.6	0.7	1.1	2.0	6.4	9.6	8.9	2.0	1.0

Table 2 continued

Elements	Al	Fe	Ca	Cu	Mo	Pb	Zn	Ni	Co	Cr	Cd	Se	As	Sb	Ba	Sr
Ef/global soils	1.6	1.3	2.2	1.3	0.7	3.9	2.3	1.7	2.3	1.1	6.5	1.1	3.4	3.5	2.0	19
Ef/carbonates	20	21	0.1	4.9	–	2.0	2.0	2.0	–	3.6	–	–	–	–	11	1.4
Ef/shale	1.7	1.8	0.3	1.2	–	1. 8	1.7	1.4	–	1.9	–	–	0.6	–	11	0.7
*I*geo/crust	− 0.1	− 0.6	− 0.9	− 1.1	− 0.6	1.1	0.1	− 1.4	− 1.1	− 0.4	0.4	2.1	2.7	2.6	0.4	− 0.5
*I*geo /global soils	0.1	− 0.2	0.5	− 0.2	− 1.1	1.4	0.6	0.1	0.6	− 0.4	2.1	− 0.5	1.2	1.2	0.4	3.7

The references include 1: Faure (1992), 2: WHO (1996), Bello et al. (2016); 3: Smith and Huyck (1999), 4: Lindsay (1979), Chen et al. (1999) and Salminen (2006)

by several soil parameters, inherited from parent materials and/or resulted from soil processes that are affected by climatic factors (Kabata-Pendias and Mokherjee 2007). The solubility of iron in weathering condition is related to Eh–pH conditions of iron oxy-hydroxides (De Vos and Tarvainen 2006). Iron is considered as one of the essential nutrients for plant growth (Kabata-Pendias 2011); therefore, the high contents of iron in the soils of the studied area may have significant safeguard effects on the growing plants. Although the solubility and availability of iron from Fe-oxy-hydroxides in ferruginous soil is low, the interaction of iron oxy-hydroxides with plant and organic substances could increase the availability of soluble Fe^{3+} complexes for plant growth (Kabata-Pendias 2011; Colombo et al. 2013). The health effect associated with deficiency of iron is anemia, and excess for the dominant exposure to this element includes ingestion, hemochromatosis, siderosis, cardiac failure, and cancer (Plumlee and Ziegler 2005).

Calcium (Ca)

Calcium is reported to be the sixth abundant (3.6%) element in the earth's crust, essential nutrient in plant growth and plays an important role in cell division and elongation (Mason and Moore 1982; Kabata-Pendias 2011). The variation of the average calcium baseline in calcareous soils, ferruginous soils, baritic soils and soils developed on shale layers appears to be 129,920, 91,101, 59,036 and 29,527 mg/kg, respectively (Table 1). These values are 3.5–6.7 times higher than the crustal abundance and global soil level (Table 2). This is supported by lognormal distribution of Ca with four different soil populations (Fig. 5c). The highest value of Ca (almost 13%), especially in association with Sr, Mg and Ba (Mielke 1979), indicates the presence of calcareous parental rocks in the studied area. This also reflects the presence of calcite, dolomite as well as minor replacement of calcium for Ba (Levinson 1980) in the structure of barite and dolomite in the soils of the area. Calcium has generally a high mobility, except under strongly alkaline conditions, occurs in solution as dissociated Ca^{2+} ions (De Vos and Tarvainen 2006), is mobile and available by the water circulation from the roots through the leaves of the plants, is considered as an essential soil fertility nutrient for plant growth and is not commonly reported to be toxic to plants (Kabata-

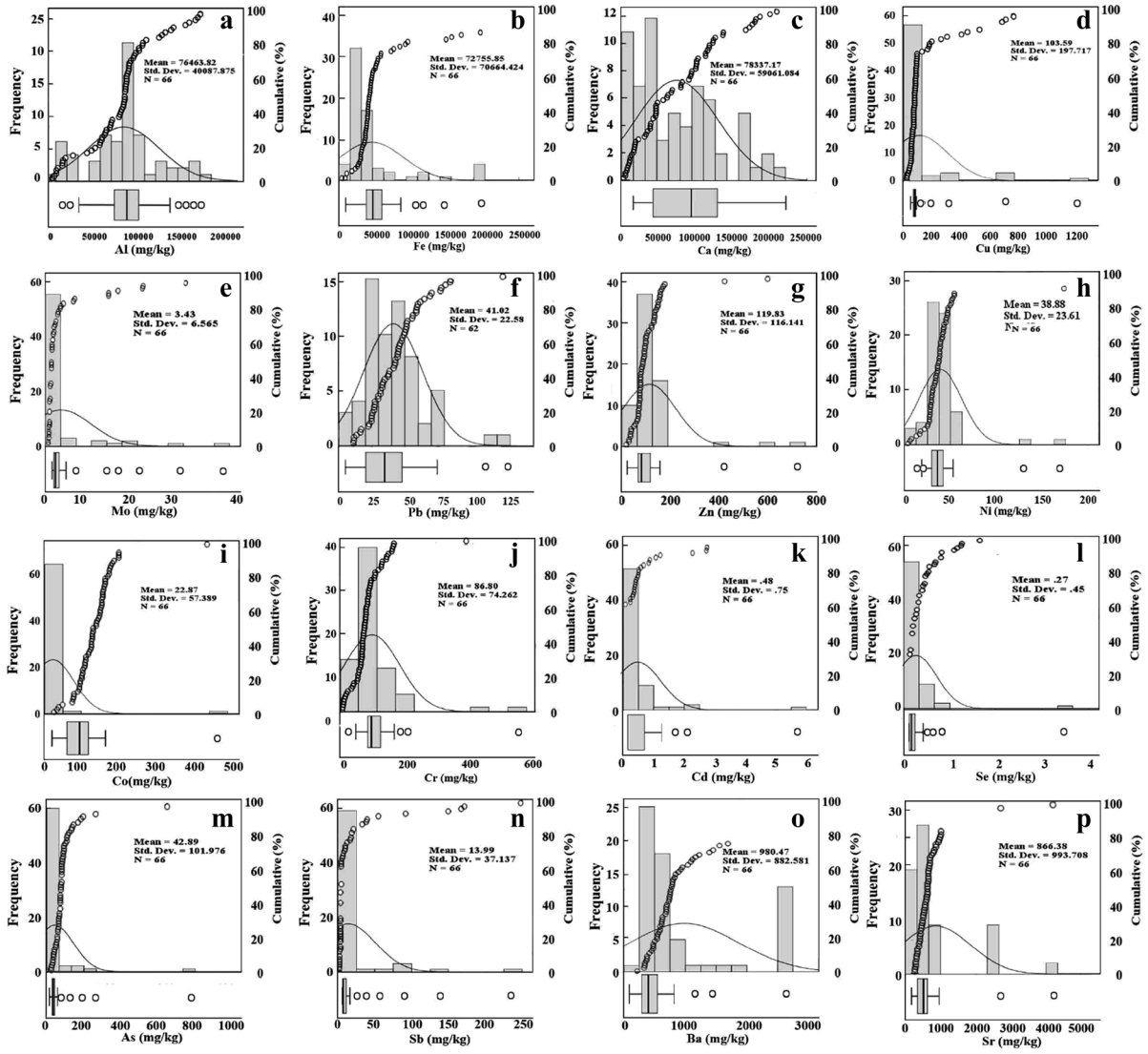

Fig. 5 Histogram, box plot and cumulative percentage diagrams of elements in all soil samples

Pendias 2011). However, excess values of Ca in soils can reduce uptake of P, K, Mg, B, Cu, Fe and Zn for plant growth (Kabata-Pendias and Mokherjee 2007). This may be a possible reason for the limitation of the stunted flora in the Baghin area. Health effects associated with the excess of prolong exposures of calcium are ingestion, atherosclerosis, cataracts and gall stones (Plumlee and Ziegler 2005).

Copper (Cu)

Copper is considered as an essential trace and heavy element in soil, plant nutrition and growth that regulates several plant enzymes (Rose et al. 1979; Kabata-Pendias 2011; Selinus 2013). The mean baseline concentrations of Cu range from 38.1 mg/kg in soils developed on shale layers to 290 mg/kg in baritic soils. Average copper values between 53 and 68 mg/kg occur in calcareous and ferruginous soils and are close to the soil and plant permissible limits (Table 2) reported by WHO (1996) and Plumlee and Logsdon (1999). It is noteworthy that only copper content in baritic soils is 5.3–9.7 times higher than the crustal abundance and average global soil level (Table 1). This could be due to the presence of chalcopyrite, malachite and azurite associated with barite and

galena in hydrothermal veins. The frequency histogram, cumulative percentage and box plot diagrams (Fig. 5d) indicate anomalous positive skewness and lognormal distribution for four soil populations. The average content of Cu in global soil varies from 13 to 24 mg/kg and is usually accumulated in the surface horizons of soils due to its uptake by organic matter (De Vos and Tarvainen 2006). Copper occurs in most soils as the $Cu(H_2O)_6^{2+}$ ion adsorbed on clay minerals or co-precipitated on other mineral and organic soil components (Kabata-Pendias and Mokherjee 2007). During chemical weathering of parent rocks and soil formation, Cu is associated with clay minerals, organic carbon and iron and manganese oxy-hydroxides. In oxidizing environments, Cu is likely to be more soluble under acidic and reducing conditions (Callender 2003). Natural attenuation of Cu occurs as an effect of Cu substituting for Ca in the structure of calcite in calcareous soils and precipitation of $Cu(OH)_2$ and/or $Cu_2(OH)_2CO_3$ in other soils (Kabata-Pendias and Mokherjee 2007). Although copper is an essential metal for plant growth, somewhat higher concentrations than the permissible levels are toxic to plants (Brooks 1972; Kabata-Pendias 2011). Since the concentration of copper in baritic soils of the studied area is higher than the global permissible levels, it is considered as an environmental concern in the area. The deficiency of copper in human causes anemia and Menke's syndrome. Excess exposure of this element includes Wilson's disease (associated with Cu buildup in organs), intestinal and liver inflammation, hemolysis (destruction of red blood cells, with diffusion of hemoglobin into surrounding fluids) and hyperglycemia (Plumlee and Ziegler 2005).

Molybdenum (Mo)

Molybdenum is a minor heavy element in soil and plant growth (Brooks 1972; Kabata-Pendias 2011). The mean baseline content of molybdenum is 1.15 mg/kg in calcareous soils and 1.45 mg/kg in soils developed on shale layers, which are lower than crustal content (Table 1). The ferruginous and baritic soils contain 6.8 and 6.2 mg/kg, respectively, 3 to 4.6 times higher than the crustal abundance and global soil content (Tables 1 and 2), although these values appear to be close to the soil and plant permissible levels. Maximum values of Mo (37 mg/kg) are reported from the baritic soils due to substitution Mo in structure of sulfides such as pyrite (De Vos and Tarvainen 2006) and chalcopyrite (Yin et al. 2017), which occur as minor sulfide minerals in hydrothermal veins of the studied area. Figure 5e shows positive skewness and lognormal distribution with two distinguished soil populations. The behavior of Mo in soils differs greatly from that of the other trace metals as it is readily mobilized in alkaline soils (pH > 6.5) (Kabata-Pendias and Mokherjee 2007). However, relatively easily soluble Mo anions are readily co-precipitated by organic matter, $CaCO_3$, Fe–Mn hydroxides. It is also adsorbed by freshly precipitated $Fe(OH)_3$ (Brooks 1972; Kabata-Pendias 2011). Although high Mo values (> 10 ppm) are moderately toxic to plants and livestock (Kabata-Pendias 2011), its low values in the studied area are not in the environmental risk level. Health effects associated with deficiency of molybdenum in human are growth depression, keratinization effects, hyperuricemia. The excess of this element leads to high uric acid in serum and urine, loss of appetite, diarrhea, slow growth, anemia, "gout-like" lesions and molybdenosis (Plumlee and Ziegler 2005).

Lead (Pb)

Lead is reported to be a toxic heavy metal in contaminated soils with severe toxicity to plants (Brooks 1972; Kabata-Pendias 2011; Selinus 2013). The mean baseline variations of Pb concentrations in different soils range from 39 mg/kg in the soils developed on shale layers to 45 mg/kg in baritic soils, which are close to the soil and plant permissible limits (Tables 1 and 2). However, the highest content of lead (130 mg/kg) is found in calcareous soils, reflecting the occurrence of galena in hydrothermal veins crosscutting the carbonate rocks. Figure 5f shows positive anomalous skewness, lognormal distribution of Pb as well as four soil populations. The high Pb values in soils are related to the presence of galena associated with barite in hydrothermal veins (Kashfi 1997). Callender (2003) and Krauskopf (1967) suggested that concentration of Pb and other trace metals in soil and sediments is controlled by adsorption onto the ferric and manganese oxy-hydroxides, clay mineral and organic matter. During weathering, Pb sulfides are slowly oxidized and have an ability to form carbonates and also to be fixed by clay minerals, Fe-oxy-

hydroxides, and soil organic matter (Kabata-pendias 2011). The extent of Pb adsorption onto hydrous Fe–Mn oxides is influenced by the physical characteristics of the adsorbent and the composition of the aqueous phase (pH, Eh and ion complexing, Kabata-pendias 2011). Since lead is a severe toxic element for plant growth, the high values of Pb in the Baghin area are of great environmental concern. Lead is not an essential element and health effects associated with excess of this element are acute poisoning, renal failure and severe distress. Chronic poisoning leads to central nervous system problems, impaired neurobehavioral function, diminished gross and fine motor development in children, kidney disease, hypertension, anemia, and other hematologic effects (Plumlee and Ziegler 2005).

Zinc (Zn)

Zinc is a minor essential heavy metal for plant growth, transports calcium through the plants and an activator for the production of the chlorophyll (Brooks 1972; Kabata-Pendias 2011; Selinus 2013). The mean baseline zinc value in baritic soils is 168 mg/kg, almost 3 magnitudes higher than crustal abundance and global soil, but similar to the permissible soil and plant limits (Table 1 and 2). Nonetheless, the average baseline for calcareous soils is 100 mg/kg zinc. The mean baseline Zn variations in ferruginous soils and the soils that develop on the shale layers are 66 mg/kg and 115 mg/kg, respectively. Figure 5g shows an anomalous positive skewness and lognormal distribution for zinc. The maximum value of Zn in the baritic soils (767 mg/kg, Table 1) is due to the presence of sphalerite (ZnS) associated with hydrothermal veins. Although Zn is very mobile in most soils, clay fractions and soil organic matter are capable of holding Zn quite strongly, especially at neutral and alkaline pH regimes (Kabata-Pendias 2011). Zinc mobility in the environment is greatest under oxidizing and acidic conditions, but more restricted under reducing conditions. The weathering of sulfide minerals in oxidizing conditions may give rise to high concentrations (> 100 ppb) of dissolved Zn sulfates and carbonates (Massey and Barnhisel 1972). At pH values above 7, aqueous complexed Zn begins to partition to particulate Zn as a result of sorption onto iron oxy-hydroxides (Callender 2003). Given the fact that Zn is a moderately toxic heavy metal (Brooks 1972; Kabata-Pendias 2011), the high values of Zn (up to 796 mg/kg) in soils of the studied area are of possible environmental concern. The deficiency of Zn is shown by anorexia, dwarfism, anemia, hypogonadism, hyperkeratosis, acrodermatitis, enteropathica, depressed immune response and teratogenic effects. The excess values of Zn cause hyperchronic anemia, and metal fume fever at high doses (Plumlee and Ziegler 2005).

Nickel (Ni)

The mean baseline value of nickel in the baritic soils is 188 mg/kg (Table 1), 7.5, 3.9 and 37 magnitudes higher than the global soil level, soil permissible limits and plant permissible limits (Tables 1 and 2), respectively, while the nickel content in the other soil samples does not show significant variations (Table 1). The frequency histogram, box plot and cumulative percentage diagrams (Fig. 5h) show anomalous positive skewness and lognormal distribution for nickel. The increase of nickel content in the baritic soils may be due to the substitution of this element in the structure of sulfides, in particular pyrite (Levinson 1980) in hydrothermal barite–galena veins. A close relationship between Ni and clay content in soils is observed, although iron oxides could adsorb Ni at pH 5.5 condition (Kabata-Pendias 2011). Nickel is a minor essential element to plant growth, plays an important role to overall nitrogen metabolism, but contaminated soils with high Ni values may cause severe toxicity to plants (Brooks 1972; Kabata-Pendias 2011). The excess of Ni leads to chronic bronchitis, emphysema, reduced lung capacity, cancers of the lungs and nasal sinus, death (due to cardiac arrest), gastrointestinal effects (nausea, cramps, diarrhea, vomiting) and also neurological effects (giddiness, weariness) (Plumlee and Ziegler 2005).

Cobalt (Co)

The average Co baselines are 14, 13, 51 and 18 mg/kg in calcareous soils, ferruginous soils, baritic soils and the soils formed on shale outcrops, respectively (Table 1). These baselines are very close to the global soil level, crustal abundance and permissible soil limits (Table 2), but almost 20 orders higher than the plant permissible limits. The mean value of cobalt in baritic soils (51 mg/kg), is two times higher than the crustal abundance (Table 1). This may be due to Co

substitution for Fe^{+3} in the structure of hematite and goethite or replacing the structure of pyrite (Levinson 1980). Figure 5i shows histogram, box plot and cumulative diagrams of Co, which illustrates a positive anomalous skewness and lognormal distribution, reflecting three populations. Several soil factors govern the Co distribution in soils of which Fe–Mn oxy-hydroxides are of the greatest importance (Kabata-Pendias 2011). Fe-oxy-hydroxides have strong affinity for the selective adsorption of Co. This is well reflected in the Co distribution in soil profiles that shows a close relation between the levels of Fe and Co in a particular soil horizon (Kabata-Pendias and Mokherjee 2007). The low values of Co in the soils of the studied area are not in the level of environmental risk. Health effects associated with deficiency of cobalt are anemia, anorexia and excess values for the dominant exposure of this element are ingestion, cardiomyopathy, hypothyroidism, polycythemia (excess of red blood cells) and cancer (Plumlee and Ziegler 2005).

Chromium (Cr)

The mean baseline chromium values in ferruginous, calcareous, and baritic soils as well as the soils developed on shale layers are 55 mg/kg, 73 mg/kg, 100 mg/kg and 114 mg/kg, respectively (Table 1). These values are almost close to the crustal abundance, global soil level and soil permissible limits, but much higher than the plant permissible limits (Table 2). During chemical weathering, the behavior of Cr^{3+} resembles that of Fe^{3+} and Al^{3+} (Mielke 1979), leading to widespread accumulation in secondary Fe-oxy-hydroxides and clays. Highly oxidized Cr^{6+} is much more mobile than Cr^{3+}, especially under very acid and alkaline ranges of pH, although readily soluble Cr^{6+} in soils is much more toxic than Cr^{3+} to both plants and animals (Kabata-Pendias and Mokherjee 2007). The toxic effects, caused by Cr^{6+} however, are highly dependent on soil properties, soil textures and pH (Kabata-Pendias and Mokherjee 2007). The frequency histogram, box plot and cumulative percentage diagrams (Fig. 5j) show anomalous positive skewness and lognormal distribution of chromium for four soil populations. The sorption of Cr in soil is associated primarily with the clay content, and to a lesser extent with Fe-oxy-hydroxides and the organic matter content. Since Cr contents of the soils in the studied area are within the global soil level, no environmental hazard is expected. Chromium (III) is an essential element for human health and has important effect on glucose metabolism. Deficiency of Cr may cause hyperlipidemia, corneal opacity. The excess of Cr causes percutaneous absorption, irritation of generation of lesions in skin, respiratory tract, gastric and intestinal mucosa, contact dermatitis, pulmonary edema, acute kidney failure and long-term risk for lung cancers (Plumlee and Ziegler 2005).

Cadmium (Cd)

The average Cd concentration in soils follows 0.4 mg/kg in ferruginous soils, 0.3 mg/kg in baritic soils, 1.0 mg/kg in calcareous soils and 0.4 mg/kg in soils developed on shale layers (Table 1), respectively, and are almost similar to the crustal abundance, global soil level, soil permissible limits and plant permissible limits (Table 2). However, few samples show positive anomalous skewness and lognormal distribution (Fig. 5k). The maximum amount of Cd (5.7 mg/kg) in baritic soils could be due to presence of sphalerite associated with baritic veins and substitution of Cd for Zn in sphalerite structure. The cationic adsorption of Cd by clay minerals and Fe oxy-hydroxides (Kabata-Pendias 2011) is another possible reason for high Cd values in ferruginous and baritic soil samples. The precipitation of Cd may occur at high Cd^{2+} activities under alkaline ($pH > 7.0$) and anaerobic conditions. As the majority of soil samples in the studied area show Cd concentration similar to those of the soil and plant permissible limits, no environmental hazard is expected. Cadmium is not an essential element, and health effects associated with the excess of this elements are acute exposure, gastroenteritis, liver–kidney damage, cardiomyopathy, metabolic acidosis, irritation of nasopharyngeal tract, and pneumonitis. Chronic exposure can lead to obstructive lung disease, bronchitis, emphysema, lung cancer, kidney damage and secondary skeletal system effects (Plumlee and Ziegler 2005).

Selenium (Se)

Selenium is a heavy metalloid with very low crustal concentration (0.05 mg/kg) and has a significant interaction with soils, plants, animals and humans,

and it is considered to be moderately toxic element (Brooks 1972; Kabata-Pendias 2011; Selinus 2013). The mean Se baselines in calcareous soils, ferruginous solis, baritic soils and the soils developed on shale layers are 0.2, 0.2, 0.4 and 0.3 mg/kg, respectively, 4–7 times more than the crustal abundance (Table 1). The maximum value (1.0 mg/kg) of Se is related to the soils developed on shale layers, which may be related to the adsorption by clay minerals (Levinson 1980). Figure 5l shows positive anomalous skewness and lognormal distribution with two populations. During chemical weathering of rocks, Se is easily oxidized and the state of its oxidation as well as its solubility is controlled by the pH–Eh soil system (Kabata-Pendias and Mokherjee 2007). A high Se mobility can be expected in soils with high pH and Eh. In alkaline Se-rich soils, the predominated Se species is Se^{6+}, which is very weakly adsorbed. Hence, selenates occur in soluble forms in soil of arid–semiarid regions (Kabata-Pendias and Mokherjee 2007). Although Se is a moderately toxic heavy metalloid in the geochemical cycle, its high values in the Baghin area may be of environmental concern. The deficiency of Se causes liver necrosis, endemic cardio-myopathy (Kesham disease), osteoarthropathy (Kashin's Beck disease) and membrane malfunction. The excess values of Se lead to birth effects fetal toxicity, liver–kidney damage, cancer, brittle hair and nails, skin lesions and selenosis (Plumlee and Ziegler 2005).

Arsenic (As)

Arsenic is a non-essential heavy metalloid that is reported to be generally toxic and carcinogenic to plants, animals and humans (Brooks 1972; Kabata-Pendias 2011; Selinus 2013). The mean arsenic baseline values in calcareous soils (26 mg/kg), ferruginous soils (30 mg/kg), baritic soils (114 mg/kg) and soils developed on shale layers (17 mg/kg) (Tables 1 and 2) are 5, 5, 22 and 3 magnitudes higher the crustal abundance, global soil level, soil permissible limits and plant permissible limits (Table 2). Importantly, the maximum arsenic values belong to the baritic soils (800 mg/kg), much higher than the maximum soil permissible level in soils (55 mg/kg) (Selinus 2013). This is reflected in histogram, box plot and cumulative diagrams of As (Fig. 5m), which illustrates a positive anomalous skewness and lognormal distribution for As. The high arsenic levels in soils could be due to the replacement of arsenic in the structure of galena and sphalerite (Levinson 1980) associated with hydrothermal barite veins. Colloidal adsorption of arsenic by clay minerals and Fe–Mn oxy-hydroxides may be the other causes for high As values in the soils. In this respect, Reimann et al. (2003) suggested that arsenic minerals and compounds are readily soluble, but arsenic migration is limited, because of the strong sorption by clays, Fe–Mn oxy-hydroxides and organic matter. Although arsenate ions are readily fixed by clays, phosphoric gels, humus and hydrated Fe oxides (goethite), the Al oxides are the most active for As retention (Kabata-Pendias 2011; Reimann et al. 2003). Since arsenic is a toxic and carcinogenic element for plants and human through soil, air and water, the high contents of arsenic in the studied soils of the area are highly of environmental concern. Arsenic is not an essential element and health effects associated with the excess of this elements are acute poisoning that can lead to a wide variety of maladies, including systemic hypotension, pain, bleeding, pulmonary edema, anemia, destruction of red blood cells, liver necrosis, kidney failure; encephalopathy and other central and peripheral nervous system disorders (Plumlee and Ziegler 2005).

Antimony (Sb)

Antimony is a heavy metalloid; its excessive concentrations in soils are of potential harm to plants, animals, and humans (Brooks 1972; Kabata-Pendias 2011; Selinus 2013). The mean Sb baseline concentrations in calcareous soils, ferruginous soils, baritic soils and the soils developed on shale layers include 9.0 mg/kg, 9.4 mg/kg, 42 mg/kg and 1.8 mg/kg, respectively, 18, 19, 84 and 3.5 magnitudes higher than the global soil value, crustal abundance, soil permissible limits and plant permissible limits (Tables 1 and 2). The maximum antimony value in baritic soils (228 mg/kg) is more than 209 magnitudes higher than the global soil level (0.5 mg/kg, Table 3). Figure 5n shows histogram, box plot and cumulative percentage diagrams of Sb, where the data show a positive anomalous skewness and lognormal distribution with three distinctive soil populations. Antimony is a chalcophile element that could replace in structure of galena and sphalerite (Levinson 1980), which are the minor associated sulfide minerals in barite veins in the studied area. In the secondary environment, Sb has

a strong tendency to sorb by Fe–Mn oxy-hydroxides, organic residues and clay minerals (Reimann et al. 2010). Antimony is a toxic heavy metalloid to plants and humans; thus, its high values in the soil of the studied area should be considered as an environmental concern.

Barium (Ba)

Barium is an alkaline earth heavy metal with a crustal abundance of 425 mg/kg, and its ingestion in soluble forms is reported to be toxic to plants, animals and human beings (Brooks 1972; Nogueira et al. 2010: CCME 2013). The mean baseline variations of barium in calcareous, ferruginous, baritic soils and the soils developed on shale layers are 564, 890, 1823 and 860 mg/kg, respectively (Table 1). The mean value of Ba in baritic soils is 4 times more than the crustal abundance and global soil level (Table 2). The frequency histogram, box plot and cumulative percentage diagrams (Fig. 5o) show anomalous positive skewness and lognormal distribution for Ba, reflecting three anomalous soil populations. The reported Ba values for soils on the world scale range from 84 to 960 mg/kg, being the lowest in organic soils and the highest in loamy and clay soils (Kabata-Pendias and Mokherjee 2007). Ba is insoluble, and it is easily precipitated as sulfate and carbonate, strongly adsorbed by clays and Mn–Fe oxy-hydroxides (Kabata-Pendias 2011). Therefore, the transport, fate and toxicity of barium in the environment are largely controlled by its solubility (Menzie et al. 2008). Despite the low solubility of barite, the Ba concentrations in soils of the Baghin area are anomalous and may be of environmental concern. In this regard, Nogueira et al. (2010) reported that among the plants, only legumes, forage plants, tomatoes, soybean and mushrooms can accumulate certain amounts of Ba. Although the toxicity of barium sulfate is slight to moderate through soils and air–water cycle, the exposure of barium compounds causes hypertension, gastrointestinal disturbances, renal function, muscular weakness, swelling of the brain and liver, high blood pressure and heart damage (Choudhury and Cary 2001; Nogueira et al. 2010). However, experiment on animals revealed no evidence of carcinogenic symptoms of Ba salts (Shahab et al. 2016).

Strontium (Sr)

Naturally occurring strontium belongs to the heavy alkaline earth elements, accumulate in soils, plants and humans (Selinus 2013). The mean baseline content of strontium follows 531 mg/kg in calcareous soils, 982 mg/kg in ferruginous soils, 1886 mg/kg in baritic soils and 388 mg/kg in the soils developed on shale outcrops (Table 1). These baseline variations in Sr are 2.6 and 5 orders higher than the crustal values, but 26, 49, 94 and 19 magnitudes more than the average global soil level. The enrichment in Sr could be due to replacement of Sr^{2+} for Ca^{2+} and Ba^{2+} in calcareous and baritic soil samples (Rose et al. 1979). Figure 5p shows anomalous positive skewness and lognormal distribution for strontium, representing background and anomalous populations. Strontium content of soils is highly controlled by parent rocks, sulfates, carbonates and climate (Kabata-Pendias 2011). Strontium is moderately mobile in soils, and the predominate Sr^{2+} is likely to be adsorbed by clay minerals and Fe-oxy-hydroxides (Kabata-Pendias 2011). It is noticeable that strontium is strongly associated with calcium and is indicative of carbonate rocks, especially in association with Sr, Mg and Ba (De Vos and Tarvainen 2006). Although limited data are available on slight toxicity of natural strontium to humans and plants, high strontium exposure to soils leads to childhood rickets (Brooks 1972; Watts and Howe 2010). Strontium in low quantities is beneficial along with Ca and vitamin D to strongly bind the bone tissues and increase bone density, thus reducing the process of osteoporosis in humans. On the contrary, cumulative consumption of high Sr (4 mg/l) may interfere with Ca in bones and often causes fractures and osteodystrophy (Shahab et al. 2016).

Other elements

According to Tables 1 and 2, the concentrations of Ti, Mg, Na, K, P, Mn, Rb, V, Li, Cs, Zr, W, Bi, Be, Ga, Ge, Nb, Sc, Y, Ce, Nd, Sm, Eu, Gd, Dy, Er and Yb in soil samples are within the soil permissible limits, plant permissible limits, crustal abundance and global soil levels and thus have no adverse environmental effects to plants, wildlife and humans.

Table 3 Pearson correlation coefficient of calcareous soils (A), ferruginous soils (B), baritic soils (C) and soils developed on shale layers (D)

Proximity matrix																
Case	Al	Fe	Ca	Cu	Mo	Pb	Zn	Ni	Co	Cr	Cd	Se	As	Sb	Ba	Sr
A																
Al	1.0	0.7	− 0.8	0.7	0.3	− 0.2	− 0.1	0.7	0.9	0.8	0.1	− 0.3	− 0.1	0.1	0.2	0.2
Fe		1.0	− 0.7	0.7	0.2	0.1	0.3	0.6	0.7	0.5	0.4	− 0.3	− 0.3	0.1	0.3	− 0.1
Ca			1.0	− 0.5	− 0.2	0.3	0.2	− 0.7	− 0.8	− 0.6	0.0	0.2	0.3	− 0.1	− 0.1	0.1
Cu				1.0	0.3	0.2	0.2	0.3	0.6	0.6	0.3	− 0.2	0.2	0.2	0.4	0.0
Mo					1.0	0.0	− 0.1	0.0	0.2	0.1	− 0.2	− 0.2	0.1	0.9	0.1	0.2
Pb						1.0	0.8	− 0.4	− 0.1	− 0.1	0.6	0.6	0.2	− 0.1	0.4	0.0
Zn							1.0	− 0.1	− 0.1	− 0.1	0.8	0.4	0.0	− 0.1	0.2	− 0.2
Ni								1.0	0.8	0.8	0.0	− 0.6	− 0.2	− 0.1	0.0	− 0.1
Co									1.0	0.9	0.1	− 0.3	− 0.1	0.0	0.3	0.1
Cr										1.0	0.1	− 0.4	0.1	− 0.1	0.3	0.1
Cd											1.0	0.2	0.2	− 0.2	0.5	0.0
Se												1.0	0.0	− 0.1	0.0	0.2
As													1.0	0.1	0.5	0.2
Sb														1.0	0.2	0.1
Ba															1.0	0.4
Sr																1.0
B																
Al	1.0	− 0.9	0.2	− 0.8	− 0.6	− 0.3	0.1	− 0.4	0.9	1.0	0.4	− 0.3	− 0.1	0.1	− 0.7	− 0.3
Fe		1.0	− 0.3	0.9	0.7	0.3	− 0.1	0.4	− 0.8	− 0.9	− 0.3	0.3	0.1	0.0	0.8	0.0
Ca			1.0	− 0.3	− 0.4	0.2	0.5	0.1	0.1	0.3	− 0.1	− 0.2	0.4	0.1	− 0.3	0.1
Cu				1.0	0.5	0.3	− 0.2	0.4	− 0.7	− 0.8	− 0.1	0.5	− 0.2	− 0.2	0.5	− 0.2
Mo					1.0	0.1	− 0.2	0.0	− 0.6	− 0.7	− 0.2	0.4	0.3	0.2	0.9	0.1
Pb						1.0	0.7	0.4	0.0	− 0.3	− 0.3	0.4	0.3	0.2	0.2	− 0.3
Zn							1.0	0.5	0.4	0.2	− 0.1	− 0.1	0.5	0.3	0.0	− 0.3
Ni								1.0	0.0	− 0.2	0.1	0.4	0.2	− 0.1	0.2	− 0.3
Co									1.0	0.9	0.4	− 0.2	0.1	0.2	− 0.5	− 0.3
Cr										1.0	0.5	− 0.3	0.0	0.0	− 0.7	− 0.3
Cd											1.0	0.1	− 0.2	− 0.2	− 0.1	− 0.2
Se												1.0	− 0.1	− 0.1	0.1	− 0.3
As													1.0	0.7	0.3	0.0

Table 3 continued

Proximity matrix																
Case	Al	Fe	Ca	Cu	Mo	Pb	Zn	Ni	Co	Cr	Cd	Se	As	Sb	Ba	Sr
Sb														1.0	0.1	0.0
Ba															1.0	0.2
Sr																1.0
C																
Al	1.0	− 0.1	− 0.1	− 0.2	− 0.1	0.4	− 0.2	0.1	0.1	0.9	− 0.1	0.1	0.0	− 0.1	− 0.7	− 0.6
Fe		1.0	− 0.6	0.4	0.5	− 0.2	0.4	0.5	0.5	− 0.2	0.4	0.4	0.4	0.3	− 0.1	− 0.2
Ca			1.0	− 0.4	− 0.4	− 0.3	− 0.4	− 0.4	− 0.4	− 0.2	− 0.3	− 0.2	− 0.3	− 0.2	0.0	0.0
Cu				1.0	0.3	0.0	0.9	0.5	0.5	− 0.2	− 0.1	0.0	0.0	− 0.1	0.1	0.2
Mo					1.0	0.1	0.3	0.0	0.0	− 0.2	0.8	0.2	0.9	0.9	0.2	− 0.2
Pb						1.0	0.1	− 0.1	− 0.1	0.6	0.1	− 0.4	0.2	0.2	0.4	0.4
Zn							1.0	0.6	0.6	− 0.2	0.1	− 0.1	0.1	0.0	0.1	0.1
Ni								1.0	1.0	− 0.1	0.2	− 0.1	0.2	− 0.1	− 0.3	− 0.2
Co									1.0	0.0	0.2	− 0.1	0.2	− 0.1	− 0.3	− 0.2
Cr										1.0	− 0.1	− 0.1	− 0.1	− 0.1	− 0.5	− 0.3
Cd											1.0	− 0.1	1.0	0.9	0.2	− 0.2
Se												1.0	− 0.1	− 0.1	− 0.4	− 0.4
As													1.0	1.0	0.2	− 0.2
Sb														1.0	0.3	− 0.1
Ba															1.0	0.9
Sr																1.0
D																
Al	1.0	0.0	− 0.5	0.4	− 0.1	0.0	− 0.1	0.5	0.5	0.7	0.2	− 0.2	0.1	0.1	− 0.4	− 0.4
Fe		1.0	0.1	− 0.5	0.1	− 0.2	− 0.2	− 0.1	0.2	− 0.3	− 0.5	0.1	0.0	0.5	0.2	− 0.1
Ca			1.0	− 0.5	0.2	0.1	0.3	− 0.2	− 0.4	− 0.6	0.1	0.3	0.0	0.1	0.5	0.2
Cu				1.0	0.1	0.5	0.4	0.5	0.4	0.6	0.5	0.2	0.3	− 0.6	− 0.3	− 0.2
Mo					1.0	0.4	0.1	− 0.5	− 0.1	− 0.3	0.1	0.5	0.3	− 0.1	0.3	− 0.2
Pb						1.0	0.6	0.1	0.4	0.1	0.4	0.4	0.0	− 0.3	− 0.1	− 0.4
Zn							1.0	0.2	0.1	− 0.1	0.7	0.1	0.2	− 0.3	0.0	− 0.2
Ni								1.0	0.5	0.7	0.2	0.0	0.0	0.0	− 0.3	− 0.1
Co									1.0	0.3	0.0	− 0.1	− 0.3	0.1	0.0	0.0
Cr										1.0	0.3	− 0.1	0.0	− 0.2	− 0.5	− 0.4
Cd											1.0	0.1	0.3	− 0.3	− 0.2	− 0.2

Table 3 continued

Proximity matrix																		
Case	Al	Fe	Ca	Cu	Mo	Pb	Zn	Ni	Co	Cr	Cd	Se	As	Sb	Ba	Sr		
Se												1.0	0.1	− 0.4	0.4	− 0.3		
As													1.0	0.0	− 0.1	− 0.1		
Sb														1.0	0.1	− 0.1		
Ba															1.0	0.6		
Sr																1.0		

Statistical approach

Statistical interpretations of geochemical data provide a better understanding of elemental associations in different soils. The statistical data analyses were calculated by SPSS and Excel software and are described as follows:

Correlation coefficients

The Pearson correlation coefficient has been applied for different elemental associations (Levinson 1980). The results of correlation coefficients are shown in Table 3. Accordingly, in calcareous soils, the positive correlation of Al with Fe (0.7), Cu (0.7), Ni (0.7), Co (0.9) and Cr (0.8) in ferruginous calcareous soils is related to the adsorption of Fe^{3+}, Fe^{2+}, Cu^{2+}, Ni^{2+}, Co^{2+}, by iron oxy-hydroxides and clay minerals. Significant correlation of iron with copper (0.7), nickel (0.6) and cobalt (0.739) is also due to the presence of iron oxy-hydroxides in the above-mentioned soils. Positive correlation of Cu–Co (0.6), Cu–Cr (0.6), Mo–Sb (0.9), Pb–Zn (0.8), Pb–Cd (0.6), Pb–Se (0.6) is reflected on their chalcophile affinity, adsorption by iron oxy-hydroxides as well as their replacements in the structure of minor sulfide minerals associated with barite veins. The Zn–Cd correlation (0.8) is probably related to the substitution of Cd in sphalerite structure. Also, correlation of Ni–Co (0.8), Ni–Cr (0.8) and Co–Cr (0.9) could be due to geochemical similarity of these elements in oxide minerals, minor sulfide minerals and/or adsorption by Fe-oxy-hydroxides (Levinson 1980). Table 3A illustrates the correlation of the chalcophile elements (Mo–Sb–As) is related to their occurrence in sulfide minerals and partly due to adsorption of Al–Co–Cr–Ni–Fe–Cu–Ba–Sr by Fe oxy-hydroxides and clay minerals. In soil samples developed on hematitic veins (Table 3B), aluminum has a strong correlation with Co (0.9) and Cr (0.9) but shows a weak correlation with most of the other elements. This may indicate the adsorption of these elements by iron oxy-hydroxides. Strong geochemical correlation between Fe–Cu (0.9), Fe–Mo (0.7), Fe–Ba (0.8), Ca–Zn (0.5), Cu–Se (0.6), Mo–Ba (0.9), Pb–Zn (0.7), Co–Cr (0.9) and As–Sb (0.7) is caused by the occurrence of minor sulfide minerals in hydrothermal veins or possibly adsorption by Fe-oxy-hydroxides (Rose et al. 1979; Levinson 1980). Elemental correlation analysis in soils derived from weathering of

hematite–barite veins shows an interesting feature (Table 3C). There is a correlation coefficient greater than 0.9 between Al–Cr, Cu–Zn, Cd–As and Cd–Sb. The correlation coefficients of Mo–As (0.8) and Mo–Sb (0.8), Mo–Cd (0.7), Zn–Ni (0.6), Zn–Co (0.6), Fe–Pb (0.5), Fe–Ni (0.5), Fe–Co (0.5) and Pb–Cr (0.5) are possibly due to cationic adsorption of these elements by Fe oxy-hydroxides (goethite, limonite) and clay minerals. In soils developed on shale layers, there is a significant correlation between Al–Cr (0.7) and Zn–Cd (0.7), Ni–Cr (0.7) Pb–Zn (0.6), and Ba–Sr (0.6), but a moderate association exists for Cu–Mo (0.6) (Table 3D). This may be related to chalcophile affinity of these elements as minor sulfide minerals in the barite veins (Rose et al. 1979; Levinson 1980; Shao et al. 2018).

Cluster analysis

Cluster analysis explains the possible similarity of the elemental groups (Fig. 6). The Pb–Zn–Cd–Se cluster (Fig. 6a) is linked to Ca in calcareous soils and possibly, indicating the presence of these elements as minor sulfide inclusions in carbonate rocks. In Fig. 6b, the associations of Al, Cr, Co, Cd, Ca are probably due to adsorption of these cations by clay minerals derived from weathering of the shale layers. The cluster association of As, Sb, Pb, Zn, Ni is possibly caused by the cationic adsorption by Fe oxy-hydroxides as well as the presence of minor sulfide minerals. The Mo–Ba–Fe–Cu–Se–Sr cluster represents the presence of minor sulfide minerals in barite-rich hydrothermal veins. The main cluster link for Ba–Sr–Ca (Fig. 6c) is due to the abundance of barium in baritic soils and the replacement of Sr^{+2} in calcite and barite. Sub-clusters of Al–Cr–Pb, Ni–Co–Cu–Zn and Cd–As–Sb–Mo–Fe–Se may indicate adsorption of these elements by clay minerals and iron oxy-hydroxides. It also could be related to the presence of minor chalcopyrite, galena and sphalerite in the barite-rich soils. Figure 6c indicates 4 elemental clusters in the soils developed on shale layers. These include Zn–Cd–Pb–As–Mo–Se, Al–Cr–Ni–Cu–Co, Fe–Se and Ba–Sr–Ca clusters (Fig. 6d), which show elemental associations that were adsorbed by clay minerals or Fe-oxy-hydroxides during soil formation.

Principal components analysis (PCA)

The results of principal component analysis (PCA) in calcareous soils (Fig. 7a) illustrate the presence of 5 major components, which include 86% of the total variance. This shows similarity of Al–Fe–Ni–Co–Cr link (34% variance) with Pb–Zn–Cd–Se–Ba link (21% variance) and Mo–Sb association (14% variance), indicating the occurrence of the above-mentioned elements as minor sulfide minerals or adsorption by Fe oxy-hydroxides in the soils. Figure 7b indicates the association of Fe–Cu–Mo–Ba (37.9% variance), Ca–Pb–Zn–Ni (37.9% variance), As–Sb link (13.7% variance), and Pb–Se link (9.0% variance), respectively. These elemental associations in soils may occur either as minor sulfide minerals or adsorbed the heavy metals by Fe oxy-hydroxides. The results of principal component analysis (PCA) in baritic soils (Fig. 7c) show the presence of 5 major components, including Mo–Cd–As–Sb (21% variance), which is probably due to the replacement of chalcophile elements in the structure of pyrite and chalcopyrite (Levinson 1980; Yin et al. 2017). Fe–Cu–Zn–Ni–Co component includes 18.77% variance and indicates the presence of minor sulfide minerals associated with barite in veins. Al–Pb–Cr link (14% variance) and Fe–Se link (8.5% variance) may suggest the substitution of Se for S in sulfide minerals and the adsorption of other elements by clay minerals and Fe oxy-hydroxides in the soils (Levinson 1980). The data of principal components analysis (PCA) in the soils developed on shale layers (Fig. 7d) include the presence of 5 major components and illustrate Al–Cu–Ni–Co–Cr (28% variance), Pb–Zn–Cd (20% variance), Fe–Sb (11% variance), Mo–Pb–Se (9.9% variance) and Ba–Sr link (8.80% variance) associations. These elemental associations possibly explain the adsorption of these elements mainly by clay minerals and/or Fe-oxy-hydroxides.

Discussion

Barite is an industrial mineral, which is used as an aggregate in cement, filler, weighting agent in petroleum drilling mud, sound reduction in engine compartments, radiation-shielding cement, glass ceramic and medical application for CT scan (Choudhury and Cary 2001). The main barite deposits are

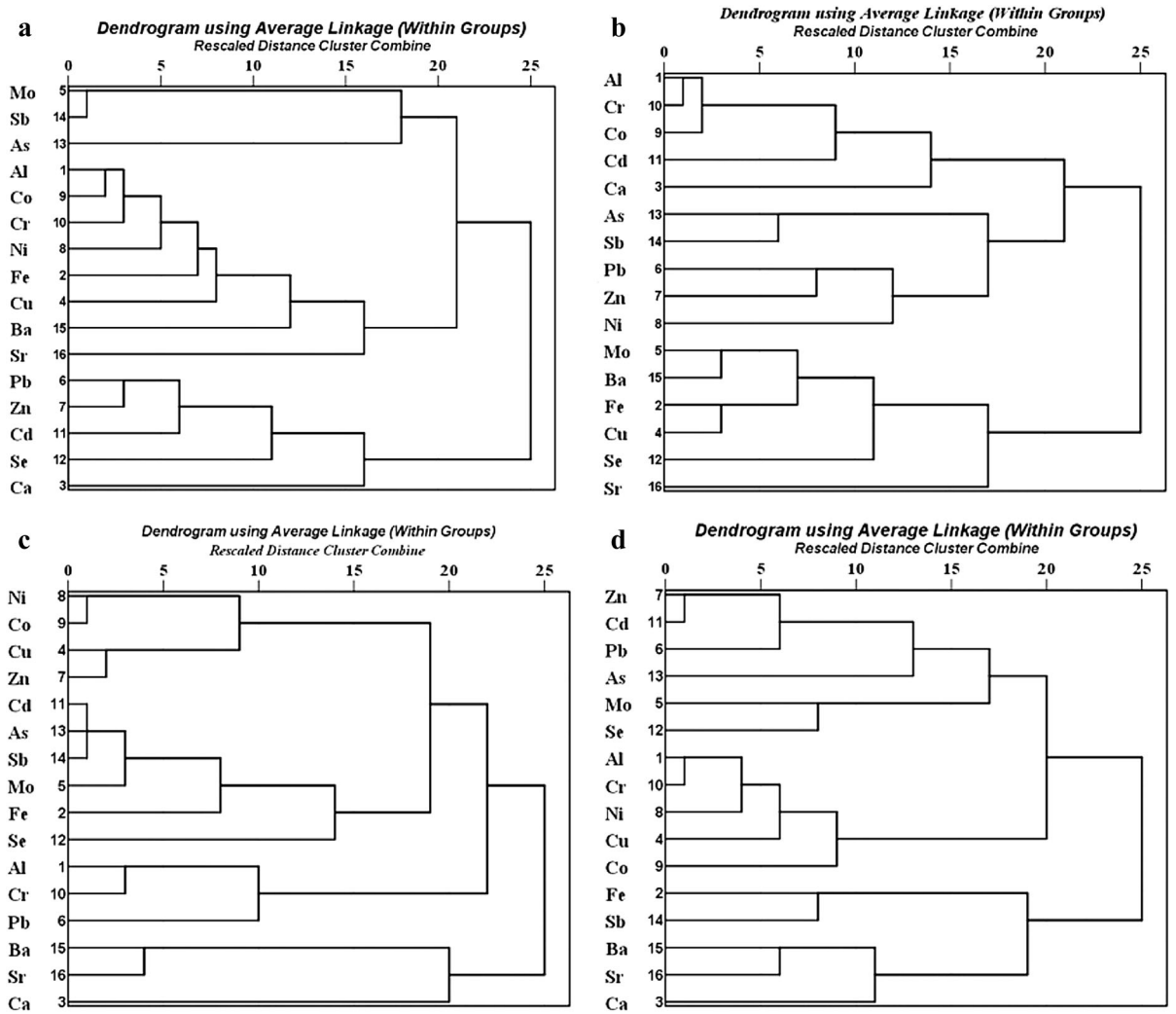

Fig. 6 Dendrograms of cluster analysis of the elements in soil samples, **a** calcareous soils, **b** ferruginous soils, **c** baritic soils and **d** soils developed on shale layers

associated with Mississippi Valley-Type ores (MVT) as well as some with SEDEX and massive sulfide mineralization (Filipek and Pumlee 1999). The chemical weathering of the above-mentioned base metal sulfide ores (pyrite, marcasite, sphalerite, galena and chalcopyrite) associated with barite ores generates acid to near-neutral waters with elevated concentrations of heavy metals and metalloid, which are of environmental concern. Despite the low solubility of barite, its associated sulfide minerals may pose serious environmental adverse effects during weathering in the geochemical cycle. This study demonstrates that barite mineralization at studied area is associated with hematite, galena and sphalerite, minor amounts of chalcopyrite and pyrite veins that crosscut the carbonate and shale host rocks. Heavy metal distribution in different soils developed over host rocks and veins gives interesting geochemical baseline for the environmental surveys in the Baghin area, and this could be generalized for similar global geological model of barite mineralization.

Among the major oxides, the concentration of SiO_2 in barite is of environmental concern. The mean content of SiO_2 in barite ore in the area is 20%wt (Kashfi 1997). This amount is higher than the limit proposed by API (2010) and reflects the presence of quartz and chert in barite veins. High SiO_2 values as quartz or other silica polymorphs cause adverse effects

a

Component Matrix

		Component				
		1	2	3	4	5
	Al	.932	.001	.021	.027	.225
	Fe	.808	.264	-.142	-.295	-.004
	Ca	-.820	.153	.119	.197	-.235
	Cu	.716	.414	.147	-.061	-.150
	Mo	.279	-.067	.816	-.453	-.068
	Pb	-.181	.917	-.022	-.149	.078
	Zn	-.080	.848	-.255	-.344	-.147
	Ni	.818	-.268	-.287	.051	-.131
	Co	.949	.041	-.085	.058	.142
	Cr	.849	.020	-.058	.346	-.026
	Cd	.148	.856	-.177	.047	-.140
	Se	-.480	.501	-.036	-.145	.607
	As	-.081	.323	.441	.591	-.428
	Sb	.138	-.079	.840	-.461	-.072
	Ba	.308	.576	.370	.387	-.021
	Sr	.031	.115	.499	.496	.585
Initial eigen values	total	5.49	3.34	2.20	1.58	1.12
	% variance	34.30	20.88	13.75	9.89	6.99
	cumulative	34.30	55.18	68.93	78.82	85.81

Extraction Method: Principal Component

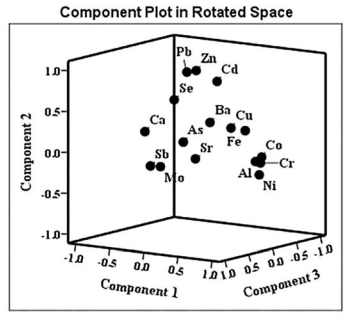

b

Component Matrix

		Component				
		1	2	3	4	5
	Al	-.973	-.127	.093	.024	.118
	Fe	.962	.046	.008	.192	-.053
	Ca	-.272	.718	.066	-.324	-.194
	Cu	.782	-.017	-.237	.431	-.053
	Mo	.763	-.284	.459	.142	.109
	Pb	.227	.583	.198	.542	-.281
	Zn	-.174	.862	.282	.184	-.004
	Ni	.314	.675	-.156	.316	.366
	Co	-.865	.122	.205	.163	.248
	Cr	-.947	.062	.011	-.004	.272
	Cd	-.291	-.068	-.155	.092	.854
	Se	.312	-.026	-.093	.718	.099
	As	.071	.442	.832	-.119	.023
	Sb	-.102	.017	.888	.022	-.210
	Ba	.811	-.073	.362	-.025	.253
	Sr	.248	-.114	-.026	-.809	-.071
Initial eigen values	total	6.06	2.95	2.18	1.44	1.01
	% variance	37.87	18.45	13.66	9.02	6.30
	cumulative	37.87	56.33	69.98	79.00	85.30

Extraction Method: Principal Component Analysis.

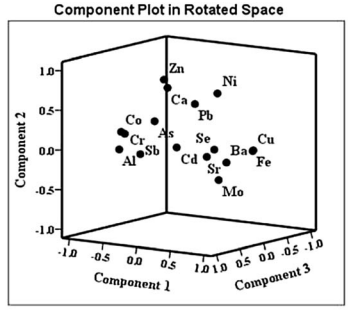

c

Component Matrix

		Component				
		1	2	3	4	5
	Al	-.057	-.040	-.568	.804	.006
	Fe	.425	.576	-.196	-.208	.464
	Ca	-.270	-.528	-.102	-.366	-.493
	Cu	-.077	.808	.317	-.050	.283
	Mo	.872	.114	.119	-.028	.366
	Pb	.144	.017	.430	.830	-.193
	Zn	.056	.879	.246	-.020	.078
	Ni	.045	.878	-.352	-.050	-.224
	Co	.061	.875	-.359	-.019	-.237
	Cr	-.113	-.105	-.295	.921	-.009
	Cd	.976	.113	-.074	-.025	-.122
	Se	-.081	-.104	-.347	-.166	.851
	As	.992	.091	-.044	.015	-.065
	Sb	.985	-.096	.103	.028	-.007
	Ba	.263	-.089	.923	-.162	-.138
	Sr	-.198	.017	.931	-.061	-.160
Initial eigen values	total	4.66	3.42	3.00	2.25	1.36
	% variance	29.11	21.39	18.77	14.07	8.53
	cumulative	29.11	50.51	69.28	83.35	91.88

Extraction Method: Principal Component Analysis.

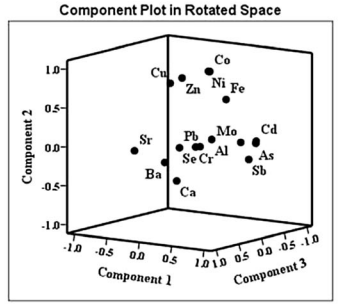

d

Component Matrix

		Component					
		1	2	3	4	5	6
	Al	.816	-.081	.140	-.069	-.313	.171
	Fe	.011	-.180	.839	.176	.071	-.120
	Ca	-.533	.449	.263	.070	.446	.055
	Cu	.629	.258	-.627	.238	-.121	.122
	Mo	-.269	.042	.051	.833	-.083	.186
	Pb	.132	.653	-.121	.549	-.254	-.246
	Zn	-.019	.950	-.144	.078	-.015	.005
	Ni	.798	.239	-.058	-.264	.041	-.039
	Co	.713	.150	.195	.117	.040	-.532
	Cr	.777	-.088	-.304	-.125	-.345	.103
	Cd	.189	.755	-.316	-.030	-.063	.370
	Se	-.018	.085	-.127	.841	.143	.019
	As	.074	.123	.012	.158	-.046	.897
	Sb	-.024	-.102	.859	-.248	-.044	.113
	Ba	-.199	-.024	.203	.332	.851	-.008
	Sr	-.165	-.153	-.152	-.281	.839	-.076
Initial eigen values	total	4.41	3.15	1.83	1.58	1.41	1.10
	% variance	27.55	19.69	11.43	9.90	8.80	6.89
	cumulative	27.55	47.23	58.66	68.56	77.36	84.25

Extraction Method: Principal Component

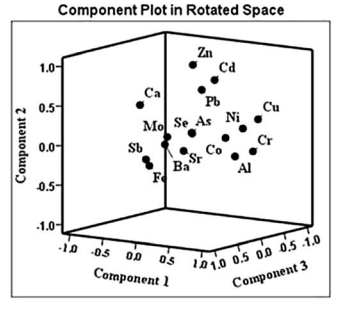

Fig. 7 Varimax-related factor for soil samples, **a** calcareous soils, **b** ferruginous soils, **c** baritic soils and **d** soils developed on shale layers

during exploration-drifting, stripping, crushing, milling and pulverization of the barite ores. It is well known (Salisu et al. 2015; Shahab et al. 2016) that prolonged exposure of fine grained silica powder or dust (< 10 μm) may cause pneumoconiosis and lung silicosis in the miners.

Figure 8 illustrates important points regarding the enrichment factor of heavy metals and metalloids in different soils. The calcareous soils (Fig. 8a) are highly enriched in Ca, Cu, Mo, Pb, Zn, Co, Cd, Se, As, Sb, Ba, and Sr, respectively. The enrichment factors are 2–50 magnitudes greater than the crustal abundance and global soil level. Among the above-mentioned elements, the chalcophile elements, particularly Pb, Cd, Se, As, Sb, and Zn, are considered to be toxic to plants, animals and humans (Lollar 2004). Furthermore, Craig et al. (2017) suggested that high values of Ba in soils inhibit growth in some terrestrial plants. The calcareous soils in the studied area are derived from the weathering of marls and carbonates. From an environmental standpoint, carbonate rocks have high neutralization potential or acid buffering potential to counteract the generation of acid mine drainage, formed by chemical weathering of sulfide minerals in Mississippi Valley-type barite ores (Filipek and Plumlee 1999). This process is conductive to the formation of near-neutral drainage waters with low heavy metal content, which reduces the heavy metals contamination into the geochemical cycle. The ferruginous soils are up to 20 magnitudes enriched in Fe, Cu, Mo, Pb, Zn, Cd, Se, As, Sb, Ba and Sr (Fig. 8b), respectively. The iron enrichment is related to the presence of iron oxides and Fe-oxy-hydroxides with a very minor contribution from sulfide minerals. The high values of chalcophile elements are released during chemical weathering of minor sulfide minerals (galena, sphalerite, chalcopyrite and pyrite) in barite veins are of environmental concern. Another factor for the enrichment of the chalcophile elements is due to the colloidal adsorption of the elements by Fe-oxy-hydroxides. With the exception of iron, which is slightly toxic, other chalcophile heavy metals and metalloids are reported to be toxic for plants, wildlife and humans through soil

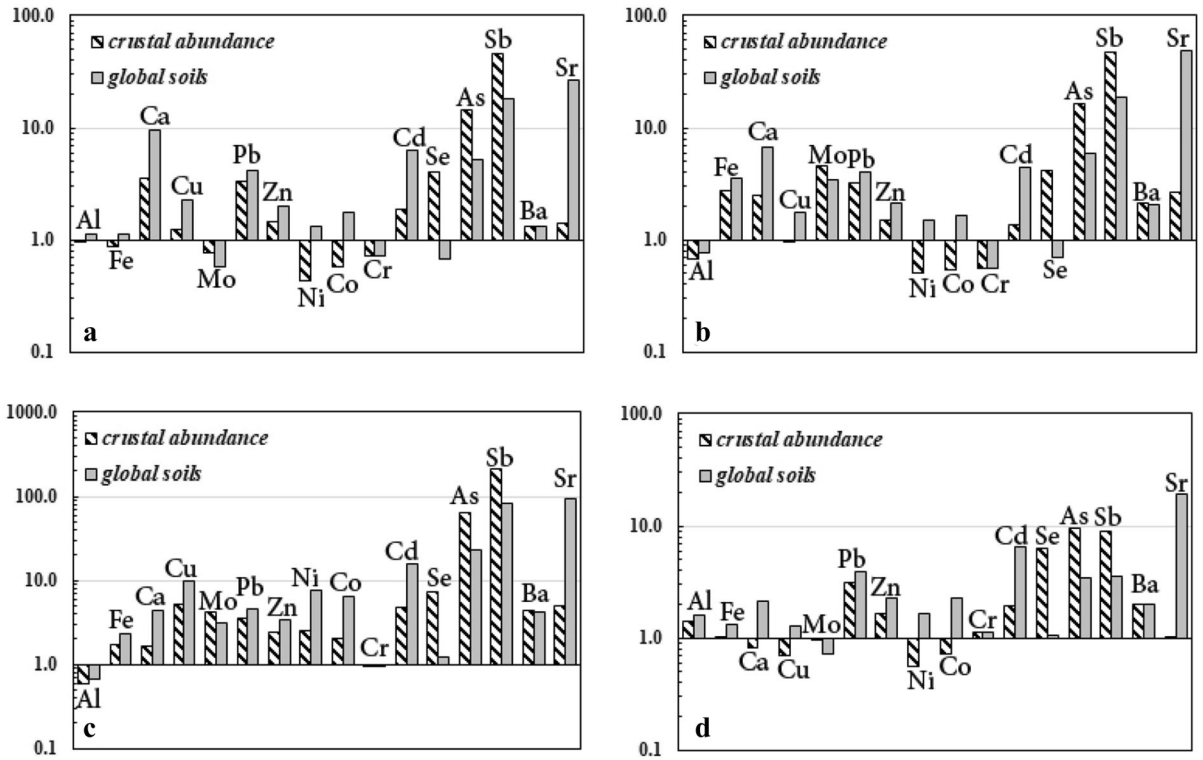

Fig. 8 Bar graph of enrichment factor normalized to crustal abundance and average global soil, **a** calcareous soils, **b** ferruginous soils, **c** baritic soils and **d** soils developed on shale layers

exposure (Brooks 1972; Kabata-Pendias 2011; Selinus 2013). Pourret et al. (2016) suggested that soils with high concentrations of Fe-oxy-hydroxides could counteract as a protective effect for reducing the toxicity of the other toxic elements. This is related to the adsorption of heavy metals by Fe-oxy-hydroxides in soils (Rose et al. 1979; Levinson 1980; Filipek and Plumlee 1999). Barite ores having iron oxides are also considered to be beneficial for drilling mud as iron oxides increase the density of the mud (Shahab et al. 2016). It is highly significant that the baritic soils are almost enriched in all elements except aluminum (Fig. 8c). This indicates the co-occurrence of minor sulfide minerals in the barite veins in the area. The high concentrations of Sr and Ca are caused by substitution of these elements in the structure of barite and calcite. In the absence of carbonate rocks, which have a high potential of neutralization (Filipek and Plumlee 1999) and depending on the abundance of sulfide minerals, these minerals could generate acid mine drainage waters with high contents of heavy metals that could have adverse effects on the environmental life. In this regard, sulfide-rich barite ores are not environmentally safe for drilling mud. In contrast to the calcareous, ferruginous and baritic soil, the soils developed on shales are moderately enriched in As, Zn, Sb, Ba, Pb and Sr (Fig. 8d), but contain high values of Al. Some high values of heavy metals are due to the adsorption by clay minerals (Kabata-Pendias 2011). One of the most remarkable roles of clay minerals is their excellent feasibility in depolluting different heavy metals that cause adverse effects in plants and humans (Kashif Uddin 2017).

One of the best criteria to show the environmental impact of different soils on plants and humans is the use of index of geoaccumulation. The index of geoaccumulation (Igeo = $\log_2$ (Cn/1.5 Bn), Muller 1969; Barbieri 2016) in soil samples of the studied areas were calculated for potentially harmful elements (Table 2). Given the fact that the host rocks in the area contain very thin veinlets of barite–galena and since there are no reports on the pre-industrial background soil values in the area, we preferred to use the crustal abundance of the elements as the soil background values. In this regard, Martinez et al. (2007) and Bam et al. (2020) considered the crustal abundance of the elements as the regional background concentration for the soil survey. The results show that the index of geoaccumulation for Sb and Sr is 3.6 and 4.1 in calcareous soils. This indicates that these elements are enriched geogenically compared to the global soil (Muller 1969). In ferruginous soils, the index of geoaccumulation for Sb and Sr is 3.7 and 5.0; thus, these elements are highly enriched. In baritic soils, the index of geoaccumulation for As, Cd, Sb, and Sr is 3.9, 3.7, 5.8 and 6.0, respectively, and these elements extremely enriched in baritic soils. Also, this index for Sr in soils developed on shale is 3.7 indicating a heavily geogenic enrichment of the soils (Table 2). However, elements differ considerably in the relative extent to which they are taken up from the soil and accumulated in plant tissues, even allowing for the differences in soil properties and plant genotype (Kabata-Pendias 2011). The soil–plant transfer of different elements varies in orders of magnitude from relatively unavailable metals such as barium to the more readily accumulated elements such as cadmium (Selinus 2013).

Overall, although the chalcophile heavy metals and metalloids are much higher than the crustal abundance, global soil level, soil permissible limits and plant permissible limits in different soils of the Baghin area, the presence of carbonate and shale host rocks possibly neutralizes and buffers the generation of acid mine waters and could conduct to the formation of near-neutral drainage waters with low heavy metals and metalloid concentrations. This is indicated by the low modal content of sulfide minerals associated with barite veins in the studied area and around several barite-bearing Mississippi Valley-Type ores (MVT) (Filipek and Plumlee 1999), although further studies on the hydrogeochemistry of the groundwater in the Baghin area are needed.

Conclusions

The soil geochemical survey in Baghin area gives the following conclusions:

1. The host rocks and hydrothermal veins are covered by calcareous, ferruginous and baritic soils and the soils developed on shale layers.
2. According to Soil Taxonomy, the soils are of entisois and the mean baseline values for Pb, As, Sb, and Sr in calcareous soils are 4–26 times more than the crustal abundance and global soil level.

3. The concentrations of Cu, Mo, Pb, Zn, Ni, Co, Cd, Se, As, Sb, Ba and Sr in baritic soils are almost more than 3 magnitudes greater than the global soil and crustal abundance.
4. The high values of chalcophile elements in soils reflect the presence of minor sulfide minerals (galena, sphalerite, chalcopyrite and pyrite) or partly are enriched by adsorption of Fe-oxy-hydroxides and clay minerals.
5. The ferruginous soils are highly enriched in Mo, Pb, Cd, As, Sb, Ba and Sr mainly due to adsorption by Fe-oxy-hydroxides.
6. Despite the low solubility of barite, minor associated sulfide minerals are possibly prone to acid mine generation and thus are of environmental concern, although this drainage-water system may be neutralized by the presence of carbonate rocks or calcareous soils.
7. The enrichment factors for Cu, Mo, Pb, Zn, Ni, Co, Cd, Se, As, Sb, Ba and Sr in baritic soil are classified as medium to heavily enriched heavy metals and metalloids by geogenic accumulation.
8. The high content of SiO_2 in barite veins is of highly environmental concern for different industrial and medical uses or drilling mud because the silica dust may trigger silicosis.

Acknowledgements The authors wish to appreciate the cooperation of Engineer M.T. Korei, former head of the Geological Survey of Iran, for continuous encouragement concerning the project. I acknowledge the help of Dr. M. Taheri for cooperation in field geology and soil sampling. We should highly appreciate the insightful comments made by Editor-In-Chief Prof. Ming H. Wong and three anonymous reviewers for their constructive suggestions.

References

Adamu, C. I., Nganje, T. N., & Edet, A. (2015). Heavy metal contamination and health risk assessment associated with abandoned barite mines in Cross River State, southeastern Nigeria. *Environmental Nanotechnology, Monitoring and Management, 3*, 10–21.

Aftabi, A. & Abbasnejad, A. (1990). *Geology, vein mineralization and mineral exploration in the Abtrosh mine, Chahamakan and Chari, Baghin region, Kerman province*. Research report. Shahid Bahonar University of Kerman. (In Persian).

Aghanabati, A. (2004). *Geology of Iran*. Tehran: Geological Survey of Iran Publication.

Alizadeh-Kouskuie, A. (2019). *Geochemical investigation on iron oxid–barite–galena mineralization and its environmental impacts in Abtorsh area, Baghin, Kerman*. M.Sc. Dissertation. Shahid Bahonar University of Kerman. (In Persian).

American National Standard (2001). *Standard practice for total digestion of sediment samples for chemical analysis of various metals*. Ann Book Stand D 4698-92.

Anonymous (2001). *Geochemical mapping of Yazd–Sabzevaran region, scale 1:100,000,* General Report. Geological Survey of Iran Publication.

API. (2010). *Petroleum and natural gas industries-recommended practice—chemical analysis of barite*. Washington DC: American Petroleum Institute.

Atapour, H., & Aftabi, A. (2002). Geomorphological, geochemical and geo-environmental aspects of karstification in the urban areas of Kerman city southeastern Iran. *Environmental Geology, 42*, 783–792.

Atapour, H. (2015). Geochemistry of potentially harmful elements in topsoils around Kerman city, southeastern Iran. *Environmental Earth Sciences, 74*(7), 5605–5624.

Bam, E. K. P., Akumah, A. M., & Bansah, S. (2020). Geochemical and chemometric analysis of soils from a data scarce river catchment in West Africa. *Environmental Research Communications, 2*, 035001.

Barbieri, M. (2016). The importance of enrichment factor (EF) and geoaccumulation index (Igeo) to evaluate the soil contamination. *Journal of Geology and Geophysics, 5*, 1–4.

Bello, S., Zakari, Y. I., Ibeanu, I. G. E., & Muhammad, B. G. (2016). Characterization and assessment of heavy metal pollution levels in soils of Dana steel limited dumpsite, Katsina state, Nigeria using geo-accumulation, ecological risk and hazard indices. *American Journal of Engineering Research (AJER), 5*(1), 49–61.

Brooks, R. R. (1972). *Geobotany and biogeochemistry in mineral exploration*. New York: Harper & Row Publishers.

Callender, E. (2003). Heavy Metals in the environment, historical trends. In B. S. Lollar (Ed.), *Environmental geochemistry* (pp. 67–105). Oxford: Elsevier-Pergamon.

CCME. (2013). *Canadian soil quality guidelines for barium: Protection of human health scientific criteria document* (p. 844). Winnipeg: Canadian Council of Ministers of the Environment.

Chen, M., Ma, L., & Harris, W. (1999). Baseline concentrations of 15 trace elements in Florida surface soils. *Journal of Environmental Quality, 28*, 1173–1181.

Choudhury, H., & Cary, R. (2001). *Barium and barium compounds: Concise international chemical assessment, document 33*. Geneva: WHO.

Colombo, C., Palumbo, G., He, J.-Z., & Cesco, S. (2013). Review on iron availability in soil: Interaction of Fe minerals, plants, and microbes. *Journal of Soils and Sediments, 14*(3), 3–9.

Craig, M. T., Zhai, H., Jaramillo, P., & Klima, K. (2017). Trade-offs in cost and emission reductions between flexible and normal carbon capture and sequestration under carbon dioxide emission constraints. *International Journal of Greenhouse Gas Control, 66*, 25–34.

De Vos, W., & Tarvainen, T. (2006). *Geochemical atlas of Europe. Part 2 Geochemistry of elements*. Geological Survey of Finland Otamedia Oy Espoo.

Dimitrijevic, M. D. (1973). *Geology of Kerman region*, Geological survey of Iran.

Djokovic, I. D., & Dimitrijevic, M. N. (1972). *Geological map of Iran, 1:100,000 series sheet 7350-Baghin*. Geological Survey of Iran.

Ehya, F. (2012). Rare earth element and stable isotope (O, S) geochemistry of barite from the Bijgan deposit, Markazi Province, Iran. *Journal of Mineralogy and Petrology, 104*, 81–93.

Faure, G. (1992). Principles and applications of inorganic geochemistry: A comprehensive textbook. Maxwell Macmillan.

Filipek, L. H., & Plumlee, G. S. (1999). Environmental geochemistry of mineral deposits: Part B, case studies and research topics. *Reviews in Economic Geology, 6B*, 583.

Galwey, A. K., Jones, K. A., Reed, R., & Dollimore, D. (1979). The blue coloration in banded fluorite (Blue John) from Castleton, Derbyshire, England. *Mineralogical Magazine, 43*, 243–250.

Ganji, A. (2015). Barite mineralization in Iran. In *Sixth balkan mining congress petrosani*. Romania.

Gholami, M. (2011). *Investigation of iron ore deposition in Estakhroeiah-Arjasb, Kuh-e-Gabri, Baghin–Rafsanjan region, Kerman province*. M.Sc. Dissertation. Shahid Bahonar University of Kerman. (In Persian).

Ghorbani, M. (2013). *The economic geology of Iran; Mineral deposits and natural resources*. Berlin: Springer.

Haji Babaei, A., & Ganji, A. (2018). Characteristics of the Ahmadabad hematite/barite deposit, Iran, studies of mineralogy, geochemistry and fluid inclusions. *Geologos, 24*, 55–68.

Hamzeh, M. A., Aftabi, A., & Mirzaee, M. (2011). Assessing geochemical influence of traffic and other vehicle-related activities on heavy metal contamination in urban soils of Kerman city, using a GIS based approach. *Environmental Geochemistry and Health, 33*, 577–594.

Huckriede, R. M., Kursten, M., & Venzalff, H. (1962). Zur geologic des Gebietes Zwischen Kerman and Sagand, Iran. *Beihefte zum Geologischen Jahrbuch, 51*, 1–197.

IAEA. (2004). *Soil sampling for environmental contaminants*. Vienna: International Atomic Energy Agency Austria.

Kabata-Pendias, A., & Mokherjee, A. B. (2007). *Trace elements from soil to human*. Heidelberg: Springer.

Kabata-Pendias, A. (2011). *Trace elements in soils and plants* (4th ed.). Boca Raton: Taylor & Fransic Press.

Kashfi, M. (1997). *Geology and mineral exploration in Abtorsh mine, Baghin region, Kerman province*. M.Sc. Dissertation. Shahid Bahonar University of Kerman. (In Persian).

Kashif Uddin, M. (2017). A review on the adsorption of heavy metals by clay minerals, with special focus on the past decade. *Chemical Engineering Journal, 308*, 438–462.

Khoshjou, A. (1999). *Barite deposits of Iran*, Geological survey of Iran. (In Persian).

Krauskopf, K. B. (1967). *Introduction to geochemistry*. Chennai: MC-Graw-Hill Book Co.

Lamb, D. T., Matanitobu, V. P., Palanisam, T., Megharaj, M., & Naidu, R. (2013). Bioavailability of barium to plants and invertebrates in soils contaminated by barite. *Environmental Science and Technology, 47*, 4670–4676.

Levinson, A. A. (1980). *Introduction to exploration geochemistry*. Wilmette, Illinois, USA: Applied publishing Ltd.

Lindsay, W. L. (1979). *Chemical equilibria in soils*. Hoboken: Wiley.

Lollar, B. S. (2004). Environmental geochemistry. In H. D. Holland & K. K. Turkian (Eds.), *Treatise on geochemistry*. Amsterdam: Elsevier.

Martinez, J., Liamas, J., De Miguel, E., Rey, J., & Hidalgo, M. C. (2007). Determination of the geochemical background in a metal mining site: example of the mining district of Linares (South Spain). *Journal of Geochemical Exploration, 94*, 19–29.

Mason, B., & Moore, C. (1982). *Principles of geochemistry*. New York: Wiley.

Massey, H., & Barnhisel, R. I. (1972). Copper, nickel and zinc released from acid coal mine spoil materials of eastern Kentucky. *Soil Science, 113*(3), 207–212.

Menzie, C. A., Southworth, B., Stephenson, G., & Feisthauer, N. (2008). The importance of understanding the chemical form of a metal in the environment: The case of barium sulfate (Barite). *Journal of Human and Ecological Risk Assessment, 14*, 974–991.

Mielke, J. E. (1979). Composition of the Earth's crust and distribution of the elements. In F. R. Siegel (Ed.), *Review of research on modern problems in geochemistry, earth science series No. 16. UNESCO Report SC/GEO/544/3* (pp. 13–37). Paris: International Association for Geochemistry and Cosmochemistry.

Muhammad, N., Zvobgo, G., & Zhang, G. P. (2018). A review: The beneficial effect of aluminum on plant growth in acid soil the possible mechanisms. *Journal of Integrative Agriculture, 17*, 60345–60347.

Muller, G. (1969). Index of geoaccumulation in sediments of the Rhine River. *Geology, 2*, 108–118.

Nogueira, T. A. R., de Melo, W. J., Fonseca, I. M., Marques, M. O., & He, Z. (2010). Barium uptake by maize plants as affected by sewage sludge in a long-term field study. *Journal of Hazardous Materials, 181*, 1148–1157.

Oden, M. I. (2012). Barite veins in the benue trough: field characteristics, the quality issue and some tectonic implications. *Environmental and Natural Resources Research, 2*(2), 21–31.

Plumlee, G. S., & Logsdon, M. J. (1999). An earth-system science toolkit for environmentally friendly mineral resource development. In G. S. Plumlee & M. J. Logsdon (Eds.), *The environmental geochemistry of mineral deposits, Part A. Processes, techniques, and health issues* (pp. 1–27)., Reviews in Economic Geology, 6A Colorado: Society of Economic Geologists.

Plumlee, G. S., & Ziegler, T. L. (2005). The medical geochemistry of dusts, soils, and other earth materials. In B. S. Lollar (Ed.), *Environmental geochemistry* (pp. 264–310). Oxford: Elsevier-Pergamon.

Porchangiz, Y. (2011). *Investigation and genesis evaluation of Bolboloeie barite mine, southeast of Kerman*. M.Sc. Dissertation. Sistan and Baluchestan University. (In Persian).

Pourret, O., Lange, B., Bonhoure, J., Colinet, G., Decrée, S., Mahy, G., et al. (2016). Assessment of soil metal distribution and environmental impact of mining in Katanga (Democratic Republic of Congo). *Applied Geochemistry, G4*, 43–55.

Rajabzadeh, M. A. (2007). A fluid inclusion study of a large MVT barite-fluorite deposit: Komshecheh, central Iran, Iranian. *Journal of Science and Technology, 31*, 73–87.

Reimann, C., Siewers, U., Tarvainen, T., Bityukova, L., Eriksson, J., Gilucis, A., et al. (2003). *Agricultural soils in Northern Europe: A Geochemical Atlas*. Stuttgart: E Schweizerbart'sche Verlags buchhandlung Stuttgart.

Reimann, C., Matschullat, J., Birke, M., & Salminen, R. (2010). Antimony in the environment: Lessons from geochemical mapping. *Applied Geochemistry, 25*, 175–198.

Rose, A. W., Hawkes, H. E., & Webb, J. S. (1979). *Geochemistry in mineral exploration* (2nd ed.). Cambridge: Academic press.

Salminen, R., Batista, M. J., Bidovec, M., Demetriades, A., De Vivo, B., De Vos, W., et al. (2005). *Geochemical atlas of Europe, part 1, background information, methodology and maps*. Espoo: Geological Survey of Finland.

Salisu, A. G., Abba, Y. B., & Mohammed, Z. (2015). Environmental and health hazards associated with exploration of barite from Bukkuyum (Zamfara State), Nigeria. *Journal of Health and Environmental Sciences, 2*, 11–15.

Selinus, O. (2013). *Essential of medical geology impact of the natural environment on public health*. New York: Springer.

Shao, Y., Wang, W., Liu, Q., & Zhang, Y. (2018). Trace element analysis of pyrite from the Zhengchong gold deposit, northeast Hunan province, China: Implications for the ore-forming process. *Minerals, 8*(262), 1–22.

Shahab, B., Bashir, E., Kaleem, M., Naseem, Sh, & Rafique, T. (2016). Assessment of barite of Lasbela, Balochistan, Pakistan, as drilling mud and environmental impact of associated Pb, As, Hg, Cd and Sr. *Environal Earth Sciences, 75*, 11–15.

Shiller, A. M., & Frilot, D. M. (1996). The geochemistry of gallium relative to aluminum in Californian streams. *Geochimica et Cosmochimica Acta, 60*(8), 1323–1328.

Simini, M., Checkal, R. T., Kuperman, R. G., Phillips, C. T., Jason, A. & Barclift, D. J. (2002). *Toxicity assessments of antimony, barium, beryllium, and manganese for development of ecological soil screening levels (ECO-SSL) using earth worm (Eisenia Fetida), Benchmark Values*. Edgewood chemical biological center Aberdeen proving ground MD.

Smith, K. S., & Huyck, H. L. O. (1999). An overview of the abundance, relative mobility, bioavailability and human toxicity of metals. In G. S. Plumlee & M. L. Logsdon (Eds.), *The environmental geochemistry of mineral deposits* (pp. 29–70). Oxford: Elsevier-Pergamon.

Suresh, S., Dinakar, N., Prasad, T. N. V. K. V., Nagajyothi, P. C., Damodharam, T., & Nagaraju, A. (2007). Effects of a barite mine on ground water quality in Andhra Pradesh, India. *Mine Water and the Environment, 26*, 119–123.

USDA. (2014). *Keys to soil taxonomy* (12th ed.). United States: Department of Agriculture.

Vlaardingen, P. L. A. van., Posthumus, R. & Posthuma-Doodeman, C. J. A. M. (2005). *Environmental risk limits for nine trace elements.* RIVM report.

Watts, P., & Howe, P. (2010). *Strontium and strontium compounds: concise international chemical assessment, document 77*. Geneva: WHO.

WHO. (1996). *Permissible limits of heavy metals in soil and plants*. Geneva: WHO.

Yin, Zh, Sun, W., Hu, Y., Zhang, Ch, Guan, Q., & Zhang, Ch. (2017). Separation of molybdenite from chalcopyrite in the presence of novel depressant 4-Amino-3-thioxo-3,4-dihydro-1,2,4-triazin-5(2H)-one. *Minerals, 7*(146), 1–19.

Zaheri-Abdehvand, N., Zarasvandi, A., Pourkaseb, H., Charchi, A., (2012). Nature of ore-forming fluid in the Farsesh Barite deposit, Southeast Aligudarz, Lorestan province. In Conference: 4th symposium of iranian society of economic geology at Birjand University, Iran.

Zarasvandi, A. R., Zaheri, N., Pourkaseb, H., Chrachi, A., & Bagheri, H. (2014). Geochemistry and fluid-inclusion microthermometry of the Farsesh barite deposit, Iran. *Geologos, 20*(3), 201–214.

Zarei, I., Pourkhabbaz, A., & Khuzestani, R. B. (2014). An assessment of metal contamination risk in sediments of Hara Biosphere Reserve, southern Iran with a focus on application of pollution indicators. *Environmental monitoring and assessment, 186*, 6047–6060.

Zienalipour-Heidarabadi, M. (2011). *Genetic evaluation and iron and barite mineralization in northeastern of Kerman province*. M.Sc. Dissertation. University of Sistan & Baluchestan, Iran. (In Persian).